

Function Aligned Regression: A Method Explicitly Learns Functional Derivatives from Data

Dixian Zhu

*Department of Genetics
Stanford University
Stanford, CA 94305, USA*

DIXIAN-ZHU@STANFORD.EDU

Livnat Jerby

*Department of Genetics
Stanford University
Stanford, CA 94305, USA*

LJERBY@STANFORD.EDU

Abstract

Regression is a fundamental task in machine learning that has garnered extensive attention over the past decades. The conventional approach for regression involves employing loss functions that primarily concentrate on aligning model prediction with the ground truth for each individual data sample, which, as we show, can result in sub-optimal prediction of the relationships between the different samples. Recent research endeavors have introduced novel perspectives by incorporating label similarity information to regression. However, a notable gap persists in these approaches when it comes to fully capturing the intricacies of the underlying ground truth function. In this work, we propose FAR (Function Aligned Regression) as a arguably better and more efficient solution to fit the underlying function of ground truth by capturing functional derivatives. We demonstrate the effectiveness of the proposed method practically on 2 synthetic datasets and on 8 extensive real-world tasks from 6 benchmark datasets with other 8 competitive baselines. The code is open-sourced at <https://github.com/DixianZhu/FAR>.

Keywords: Regression, Functional Derivatives

1. Introduction

As one of the most fundamental tasks in Machine Learning (ML) field, regression stands out as a powerful tool for understanding and modeling the relationships from complex data features to continuous data labels. Regression techniques have been widely utilized in many areas, such as computer vision (Moschoglou et al., 2017; Niu et al., 2016), drug discovery (Dara et al., 2022), economics and finances (Benkraiem and Zopounidis, 2021), environmental forecast (Zhu et al., 2018), material science (Stanev et al., 2018). Since centuries ago, Mean Squared Error (MSE) and Mean Absolute Error (MAE) have been adopted to measure the distance from the ML model predictions to the ground truths. Therefore, researchers naturally propose to optimize the least squared error and least absolute error (Legendre, 1806; Dodge, 2008). Since the last century, in order to improve the model stability and control model complexity, researchers propose different model regularization based on MSE loss, which provides multiple variants such as Ridge Regression, LASSO and Elastic Net (Tikhonov

et al., 1943; Tibshirani, 1996; Zou and Hastie, 2005). Along this line, Huber loss is proposed to trade-off the MAE and MSE, which aims to mitigate the issue that MSE is sensitive to the outliers (Huber, 1992). All these conventional loss functions and many of their variants focus on minimizing the delta between model prediction and ground truth for each individual data sample, but do not explicitly model and optimize the relationships for different data samples.

More recent studies have proposed to incorporate the label pairwise similarities with regression across different data samples, which fill a little of the gap that the conventional loss only focuses on individual prediction error (Gong et al., 2022; Keramati et al., 2023; Zha et al., 2023). However, most of the methods heuristically approximate the label similarity information as a relative rank or order given an anchor data, and hereby could lose part of the original similarity information. Besides of the potential approximation error, they have higher computational cost when comparing with the conventional loss because they need compute pairwise similarities that requires quadratic time regarding to the training batch size. There are also extensive efforts to improve regression under different learning settings, such as online learning (Pesme and Flammarion, 2020), active learning (Holzmüller et al., 2023), learning with imbalanced dataset (Yang et al., 2021; Ren et al., 2022), which are beyond the scope of this work.

Our contributions can be summarized in three main aspects: 1) we discover the caveat that the conventional regression loss has restricted narrow scope that only focus on optimizing the individual predicted value to be as close as possible to the ground truth; and thereby build the bridge from learning the functional derivatives to learning the pairwise label similarity. 2) we further propose an equivalent and more efficient formulation for learning the pairwise similarities, which only requires linear time regarding to the training batch size (as fast as conventional loss). 3) we demonstrate the effectiveness of the proposed Functional Alignment Regression (FAR) method on both synthetic datasets and 8 real-world regression tasks.

2. Related Work

Regression on Generic Setting: MSE, MAE and Huber Loss are the most common regression loss functions that work on generic regression settings (Legendre, 1806; Dodge, 2008; Huber, 1992), all of which focus on fitting the prediction to the truth for each individual data sample. There are other less exposed loss for generic regression, such as Rooted Mean Squared Error (RMSE) loss and Root Mean Squared Logarithmic Error (RMSLE) loss (Ciampiconi et al., 2023), but they are also restricted to minimizing individual error. Different regularization such as 1-norm, 2-norm penalties on model parameters have been studied as a promising way to prevent model over-fitting and improving training stability (Tikhonov et al., 1943; Tibshirani, 1996; Zou and Hastie, 2005). Extensive researches have been conducted to improve the regularization for regression by making the penalty weight adaptive or optimal under certain conditions (Zou, 2006; Wu and Xu, 2020).

Regression on Extensive Settings: when the data label is discrete, ordinal regression techniques can be applied to convert the regression task to either multiple binary classification tasks or one multi-class classification task (Niu et al., 2016; Rothe et al., 2015; Zhang et al., 2023). When learning on time-series data, researchers can apply advanced ML models, such as Recurrent Neural Network (RNN), Long short-term memory (LSTM) network or Attention model, for capturing the time-series pattern (Rumelhart et al., 1986; Hochreiter

and Schmidhuber, 1997; Vaswani et al., 2017); or, apply consecutive regularization that enhances the similarities for the predictions from adjacent time slots (Zhu et al., 2018). Researchers propose to minimize penalties for regression on multi-task learning when there are multiple tasks or targets from the dataset (Solnon et al., 2012); adapt regression to active learning when there is unlabeled data available for querying and labeling (Holzmüller et al., 2023); improving robustness for regression for online learning when the data is sequentially available (Pesme and Flammarion, 2020); improving the robustness for regression when the data is imbalanced (Yang et al., 2021; Ren et al., 2022).

Regression with Label Similarities: recently, there are several researches are proposed to improving regression with label similarities (Gong et al., 2022; Zha et al., 2023; Keramati et al., 2023). The RankSim is proposed to convert the label similarity for other data as ranks for given an anchor data; then enforce the prediction follows the same rank by add a MSE loss with the prediction rank versus the label rank (Gong et al., 2022). The RNC is inspired by contrastive learning, which follows the similar fashion as SimCLR (Chen et al., 2020), but defines the positive and negative pairs by choosing different anchor data points; RNC is proposed for pre-training that requires linear probe or fine tuning afterwards (Zha et al., 2023). ConR is also proposed in contrastive learning fashion, whose positive pairs are decided by the data pairs with high label similarities and negative pairs are decided by the data pairs with high label similarities but low prediction similarities (Keramati et al., 2023). In contrast, we propose FAR that: 1) preserves the original similarity information rather than approximate it by rank or order. 2) avoid the pairwise computation. 3) bridge FAR with learning the function derivatives which reflects pairwise relationship.

3. Method

Denote the underlying ground truth function for target $y \in \mathbb{R}^1$ on data $\mathbf{x} \in \mathbb{R}^d$ as $\mathcal{Y}(\mathbf{x})$; training dataset as $D = \{(\mathbf{x}_1, y_1), \dots, (\mathbf{x}_n, y_n)\}$, where $y_i = \mathcal{Y}(\mathbf{x}_i)$, which is sampled from underlying data distribution $(\mathbf{x}, \mathcal{Y}(\mathbf{x})) \in \mathcal{D}$. The regression task is to learn a good function $f(\mathbf{x})$ that can approximate $\mathcal{Y}(\mathbf{x})$. It is straightforward to extend the single-dimensional scalar target case to multi-dimensional target case. For the sake of simplicity, the description in this paper focuses on the single target form.

The conventional regression task optimizes the following objective:

$$\mathcal{L}_c = \frac{1}{N} \sum_{i=1}^N \ell(f(\mathbf{x}_i), y_i) \quad (1)$$

where $\ell(\cdot, \cdot)$ denote the individual loss function for each data sample. Take well-known examples, absolute error: $\ell_1(f(\mathbf{x}_i), y_i) = |f(\mathbf{x}_i) - y_i|$, squared error $\ell_2(f(\mathbf{x}_i), y_i) = (f(\mathbf{x}_i) - y_i)^2$.

3.1 Function Aligned Regression (FAR)

Besides of fitting the predicted value $f(\mathbf{x}_i)$ to be close to $\mathcal{Y}(\mathbf{x}_i) = y_i$, i.e. $f(\mathbf{x}) \approx \mathcal{Y}(\mathbf{x}), \forall (\mathbf{x}, \mathcal{Y}(\mathbf{x})) \in \mathcal{D}$, we additionally make the model to capture functional derivatives information, i.e. $\nabla f(\mathbf{x}) \approx \nabla \mathcal{Y}(\mathbf{x})$, and also for other higher order derivatives such as

$\nabla^2 f(\mathbf{x}) \approx \nabla^2 \mathcal{Y}(\mathbf{x})$. The derivatives of ground truth, $\nabla^k \mathcal{Y}(\mathbf{x})$, $k = \{1, 2, \dots\}$, are usually not available. Therefore, we derive the following corollary to help us to achieve the approximation.

Corollary 1 *For two K -order differentiable functions with open domain $f(\cdot) : \mathbb{R}^d \rightarrow \mathbb{R}^1$, $\mathcal{Y}(\cdot) : \mathbb{R}^d \rightarrow \mathbb{R}^1$, $f(\mathbf{x}_1) - f(\mathbf{x}_2) = \mathcal{Y}(\mathbf{x}_1) - \mathcal{Y}(\mathbf{x}_2)$, $\forall (\mathbf{x}_1, \mathcal{Y}(\mathbf{x}_1)), (\mathbf{x}_2, \mathcal{Y}(\mathbf{x}_2)) \in \mathcal{D}$, iff $\nabla^k f(\mathbf{x}) = \nabla^k \mathcal{Y}(\mathbf{x})$, $\forall (\mathbf{x}, \mathcal{Y}(\mathbf{x})) \in \mathcal{D}$, $k = \{1, 2, \dots, K\}$.*

Remark: it is not difficult to be proved with Mean Value Theorem. We include proof in the Appendix A.1 for the sake of soundness. It is worth noting that: $f(\mathbf{x}) = \mathcal{Y}(\mathbf{x})$, $\forall (\mathbf{x}, \mathcal{Y}(\mathbf{x})) \in \mathcal{D} \implies f(\mathbf{x}_1) - f(\mathbf{x}_2) = \mathcal{Y}(\mathbf{x}_1) - \mathcal{Y}(\mathbf{x}_2)$, $\forall (\mathbf{x}_1, \mathcal{Y}(\mathbf{x}_1)), (\mathbf{x}_2, \mathcal{Y}(\mathbf{x}_2)) \in \mathcal{D}$, but the other direction doesn't hold. For the conventional regression approaches that makes $f(\mathbf{x}) \approx \mathcal{Y}(\mathbf{x})$, $\forall (\mathbf{x}, \mathcal{Y}(\mathbf{x}))$; they may implicitly make $f(\mathbf{x}_1) - f(\mathbf{x}_2) \approx \mathcal{Y}(\mathbf{x}_1) - \mathcal{Y}(\mathbf{x}_2)$, $\forall (\mathbf{x}_1, \mathcal{Y}(\mathbf{x}_1)), (\mathbf{x}_2, \mathcal{Y}(\mathbf{x}_2)) \in \mathcal{D}$, but the objective for learning the function pairwise difference (derivatives) can be sub-optimal (more examples and insights are elaborated later on the remarks after Theorem 3 and on Fig 1, 2). Hence, we propose FAR as a direct and explicit approach that balances and optimizes the derivative discrepancy.

We propose to include the following loss of pairwise-difference objective for regression task:

$$\mathcal{L}_{\text{diff}} = \frac{1}{N^2} \sum_{i=1}^N \sum_{j=1}^N \ell(f(\mathbf{x}_i) - f(\mathbf{x}_j), \mathcal{Y}(\mathbf{x}_i) - \mathcal{Y}(\mathbf{x}_j)) \quad (2)$$

where ℓ is defined similarly as conventional regression.

Corollary 2 *Denote $\sigma_{\mathbf{x}}^f = \sigma(f(\mathbf{x}), \mathcal{Y}(\mathbf{x})) = f(\mathbf{x}) - \mathcal{Y}(\mathbf{x})$ as the deviation of prediction to ground truth. When $\mathcal{L}_{\text{diff}}$ takes p -norm loss ($\|\cdot\|_p^p$) for the N^2 elements, it has the equivalent formulation:*

$$\mathcal{L}_{\text{diff}} = \frac{1}{N^2} \sum_{i=1}^N \sum_{j=1}^N \ell(\sigma_{\mathbf{x}_i}^f, \sigma_{\mathbf{x}_j}^f) \quad (3)$$

The proof is straightforward and is included in the Appendix A.2.

Theorem 3 *When choose individual loss ℓ as $\frac{1}{2}$ squared error function, for conventional regression loss, recall Mean Squared Error (MSE):*

$$\mathcal{L}_c^{\text{MSE}} = \frac{1}{N} \sum_{i=1}^N (\sigma_{\mathbf{x}_i}^f)^2 \quad (4)$$

For the loss of pairwise difference:

$$\mathcal{L}_{\text{diff}}^{\text{MSE}} = \text{Var}(\sigma_{\mathbf{x}}^f) \quad (5)$$

where $\text{Var}(\cdot)$ denote the empirical variance.

The proof is included in Appendix A.3.

Remark:

- the conventional regression minimizes the magnitude of $\sigma_{\mathbf{x}}^f$; the loss of pairwise-difference minimizes the variances of $\sigma_{\mathbf{x}}^f$.
- A model f with smaller magnitude of $\sigma_{\mathbf{x}}^f$ might have smaller $\text{Var}(\sigma_{\mathbf{x}}^f)$, but it is not necessary. For example, $\sigma_{\mathbf{x}}^{f_1} = \{1, -1, 1, -1\}$, $\sigma_{\mathbf{x}}^{f_2} = \{10, 10, 10, 10\}$.
- On the other hand, only optimizing $\mathcal{L}_c^{\text{MSE}}$ may also trap in a sub-optimal solution regarding to both magnitude and variance of $\sigma_{\mathbf{x}}^f$. For example, $\sigma_{\mathbf{x}}^{f_1} = \{1, -1, 1, -1\}$, $\sigma_{\mathbf{x}}^{f_2} = \{1, 1, 1, 1\}$. $\mathcal{L}_c^{\text{MSE}}$ doesn't impose any preference over f_1 and f_2 , but f_2 enjoys smaller variance of deviation.
- As shown in E.q. 6, $\mathcal{L}_{\text{diff}}^{\text{MSE}}$ can be extracted as the variance component that is upper bounded by $\mathcal{L}_c^{\text{MSE}}$.

Decouple the MSE loss (denote $\bar{\cdot}$ as empirical mean):

$$\begin{aligned}
 \mathcal{L}_c^{\text{MSE}} &= \frac{1}{N} \sum_{i=1}^N (\sigma_{\mathbf{x}_i}^f)^2 = \frac{1}{N} \sum_{i=1}^N (\sigma_{\mathbf{x}_i}^f - \bar{\sigma}_{\mathbf{x}}^f + \bar{\sigma}_{\mathbf{x}}^f)^2 \\
 &= \frac{1}{N} \sum_{i=1}^N [(\sigma_{\mathbf{x}_i}^f - \bar{\sigma}_{\mathbf{x}}^f)^2 + (\bar{\sigma}_{\mathbf{x}}^f)^2] \\
 &= \text{Var}(\sigma_{\mathbf{x}}^f) + (\bar{\sigma}_{\mathbf{x}}^f)^2
 \end{aligned} \tag{6}$$

The conventional MSE loss can be decoupled to be variance and mean terms for prediction deviation, Where consequently $\mathcal{L}_c^{\text{MSE}} = \mathcal{L}_{\text{diff}}^{\text{MSE}} + (\bar{\sigma}_{\mathbf{x}}^f)^2$.

Or similarly, $\mathcal{L}_c^{\text{MSE}} = \frac{1}{N} \sum_{i=1}^N (|\sigma_{\mathbf{x}_i}^f|)^2 = \text{Var}(|\sigma_{\mathbf{x}}^f|) + (\overline{|\sigma_{\mathbf{x}}^f|})^2 = \text{Var}(|\sigma_{\mathbf{x}}^f|) + (\mathcal{L}_c^{\text{MAE}})^2$, where $\mathcal{L}_c^{\text{MAE}}$ is denoted as Mean Absolute Error (MAE).

Remark:

- $(\mathcal{L}_c^{\text{MAE}})^2 = \text{Var}(\sigma_{\mathbf{x}}^f) - \text{Var}(|\sigma_{\mathbf{x}}^f|) + (\bar{\sigma}_{\mathbf{x}}^f)^2$, there are some pairwise difference terms $(\sigma_{\mathbf{x}_1}^f, \sigma_{\mathbf{x}_2}^f$ with the same sign) expanded from $\text{Var}(\sigma_{\mathbf{x}}^f) - \text{Var}(|\sigma_{\mathbf{x}}^f|)$ can be canceled. $(\mathcal{L}_c^{\text{MAE}})^2$ only pushes the pairwise difference for $(\sigma_{\mathbf{x}_1}^f \sigma_{\mathbf{x}_2}^f) < 0$ to be larger, which makes the deviations for prediction and ground truth more sign-consistent ($\sigma_{\mathbf{x}}^f$ with the same sign for each sample). On the other hand, $\mathcal{L}_{\text{diff}}$ is proposed to solely make the deviations to be similar regardless of the magnitude.
- Although MSE implicitly captures derivative information, it lacks of flexibility to trade off the learning between the global mean functional value and local derivative values. Moreover, the global deviation $\bar{\sigma}_{\mathbf{x}}^f$ can be easily captured by a model bias parameter, which should not be treated equally with $\mathcal{L}_{\text{diff}}^{\text{MSE}}$.

Corollary 4 *When ℓ is squared error, the loss of pairwise-difference has the following simpler and more efficient empirical form:*

$$\mathcal{L}_{\text{diff}}^{\text{MSE}} = \frac{1}{N} \sum_{i=1}^N ((f(\mathbf{x}_i) - \bar{f}) - (y_i - \bar{y}))^2 \tag{7}$$

The corollary directly comes from Theorem 3 by the definition of variance.

Functional derivatives for the fitting function $\nabla^k f(\mathbf{x})$ are not always in the same magnitude of the underlying ground-truth function $\nabla^k \mathcal{Y}(\mathbf{x})$. In that case, we still want to enforce the ‘functional shape’ (or ‘normalized derivatives’) to be close, i.e. $\nabla^k f(\mathbf{x}) = C \cdot \nabla^k \mathcal{Y}(\mathbf{x})$. As a consequence, empirically:

$$f(\mathbf{x}_i) - f(\mathbf{x}_j) = C \cdot [\mathcal{Y}(\mathbf{x}_i) - \mathcal{Y}(\mathbf{x}_j)]$$

Denote the functional pairwise difference as $df_{i,j} = f(\mathbf{x}_i) - f(\mathbf{x}_j)$ and $d\mathcal{Y}_{i,j} = \mathcal{Y}(\mathbf{x}_i) - \mathcal{Y}(\mathbf{x}_j)$ for the fitting function and the underlying ground truth. The vector arrangements for them as $\mathbf{df} = [df_{1,1}, df_{1,2}, \dots, df_{N,N-1}, df_{N,N}]$, $\mathbf{dY} = [d\mathcal{Y}_{1,1}, d\mathcal{Y}_{1,2}, \dots, d\mathcal{Y}_{N,N-1}, d\mathcal{Y}_{N,N}]$. We proposed a p-norm loss function for the **normalized** pairwise difference for capturing the ‘functional shape’, denote $\|\cdot\|_p$ as p-norm:

$$\mathcal{L}_{\text{diffnorm}} = \left\| \frac{\mathbf{df}}{\|\mathbf{df}\|_p} - \frac{\mathbf{dY}}{\|\mathbf{dY}\|_p} \right\|_p^p \quad (8)$$

Corollary 5 When choose $p = 2$ for $\mathcal{L}_{\text{diffnorm}}$, we can recover negative Pearson correlation coefficient:

$$\begin{aligned} \mathcal{L}_{\text{diffnorm}}^{p=2} &= \frac{1}{2N} \sum_{i=1}^N \left(\frac{(f(\mathbf{x}_i) - \bar{f})}{\sqrt{\text{Var}(f)}} - \frac{(y_i - \bar{y})}{\sqrt{\text{Var}(y)}} \right)^2 \\ &= 1 - \frac{\text{Cov}(f, y)}{\sqrt{\text{Var}(f) \text{Var}(y)}} \\ &= 1 - \rho(f, y) \end{aligned} \quad (9)$$

where $\text{Cov}(\cdot, \cdot)$ denotes covariance and $\rho(\cdot, \cdot)$ denotes Pearson correlation coefficient.

We include the proof in the Appendix A.4.

Now that we have three components that are important for fitting regression model: \mathcal{L}_c , $\mathcal{L}_{\text{diff}}$, and $\mathcal{L}_{\text{diffnorm}}$, which are motivated to capture functional values, functional derivatives, functional shapes. Next, we propose a robust approach to reconcile them.

3.2 Robust Reconciliation for FAR

Given the huge diversity of the dataset and model, it is time-consuming to tune the three terms with exhaustive convex combination. Furthermore, the magnitude for each term can be different, which adds more difficulty to balance them. For example, $\mathcal{L}_{\text{diffnorm}}^{p=2} \in [0, 2]$ but $\mathcal{L}_c^{\text{MAE}}$ can be infinitely large; therefore, $\mathcal{L}_{\text{diffnorm}}^{p=2}$ could be easily overwhelmed when combining other components with larger magnitudes, e.g. $\mathcal{L} = (\mathcal{L}_c^{\text{MAE}} + \mathcal{L}_{\text{diff}}^{\text{MSE}} + \mathcal{L}_{\text{diffnorm}}^{p=2})/3$. For such case, consider the two solutions f_1, f_2 , where $\mathcal{L}(f_1) < \mathcal{L}(f_2)$ and $\mathcal{L}_c^{\text{MAE}}(f_1) < \mathcal{L}_c^{\text{MAE}}(f_2)$ but $\mathcal{L}_{\text{diffnorm}}^{p=2}(f_1) > \mathcal{L}_{\text{diffnorm}}^{p=2}(f_2)$. Even though the improvement for f_1 over MAE is negligible under the magnitudes, i.e. $\frac{\mathcal{L}_c^{\text{MAE}}(f_2) - \mathcal{L}_c^{\text{MAE}}(f_1)}{\mathcal{L}_c^{\text{MAE}}(f_2) + \mathcal{L}_c^{\text{MAE}}(f_1)} \approx 0$, f_1 is still a better solution as far as the overall loss is smaller.

One intuitive way for amplifying the significance of $\mathcal{L}_{\text{diffnorm}}^{p=2}$ is geometric mean, i.e. $\mathcal{L} = (\mathcal{L}_c^{\text{MAE}} \mathcal{L}_{\text{diff}}^{\text{MSE}} \mathcal{L}_{\text{diffnorm}}^{p=2})^{1/3}$, where the decreasing ratio for each component contributes equally

to the overall loss. However, it could bring another issue. Consider $\mathcal{L}(a, b, c) = (abc)^{1/3}$, $\frac{\partial \mathcal{L}(a, b, c)}{\partial a} = \frac{(bc)^{1/3}}{a^{2/3}}$. The smaller component can get larger gradient but may get numerical issue when $a \ll bc$. As a consequence, the overall objective could solely focuses on the smallest component.

Inspired by the previous two intuitive examples (the loss with smaller magnitude either gains too less attention or too much attention), we propose the a robust reconciliation approach for FAR based on a variant of Distributionally Robust Optimization (DRO) (Zhu et al., 2023), which can not only trade off the previous two cases but also only requires 1 tuning hyper-parameter (notice that a 3-term-convex-combination requires 2 tuning hyper-parameters). For each sub-loss, we apply logarithm transformation for reducing magnitude effect. For the sake of generality, we denote the individual sub-losses as \mathcal{L}_i and the overall loss as $\mathcal{L}_{\text{FAR}}(\mathcal{L}_1, \dots, \mathcal{L}_M)$, where the overall loss is composed with M sub-losses. Denote $D(\mathbf{p} | \frac{1}{M})$ as divergence measure from probability vector \mathbf{p} over simplex Δ_M to the uniform distribution $\frac{1}{M}$. The DRO formulation for FAR takes the balance from the averaged logarithm value to the maximal logarithm value:

$$\mathcal{L}_{\text{FAR}}(\mathcal{L}_1, \dots, \mathcal{L}_M; \alpha) = \max_{\mathbf{p} \in \Delta_M} \sum_{i=1}^M p_i \log \mathcal{L}_i - \alpha D(\mathbf{p} | \frac{1}{M}) \quad (10)$$

where $\alpha \geq 0$ is the robust hyper-parameter for FAR.

Theorem 6 *When take $D(\cdot | \cdot)$ as KL-divergence, FAR has the following equivalent formulation:*

$$\mathcal{L}_{\text{FAR}}^{\text{KL}}(\mathcal{L}_1, \dots, \mathcal{L}_M; \alpha) = \alpha \log \left(\frac{1}{M} \sum_{i=1}^M \mathcal{L}_i^{1/\alpha} \right) \quad (11)$$

It is worth noting that:

$$\exp \left(\mathcal{L}_{\text{FAR}}^{\text{KL}}(\mathcal{L}_1, \dots, \mathcal{L}_M; \alpha) \right) = \left(\frac{1}{M} \sum_{i=1}^M \mathcal{L}_i^{1/\alpha} \right)^\alpha = \begin{cases} (\prod_{i=1}^M \mathcal{L}_i)^{\frac{1}{M}}, & \alpha \rightarrow +\infty. \\ \frac{1}{M} \sum_{i=1}^M \mathcal{L}_i, & \alpha = 1. \\ \arg \max_{i=1}^M \mathcal{L}_i, & \alpha \rightarrow 0. \end{cases} \quad (12)$$

which trade off from geometric mean, arithmetic mean and the maximal value for $\mathcal{L}_1, \dots, \mathcal{L}_M$.

Remark: the proof is included in the Appendix A.5.

Next, we discuss how to take care of extreme case for \mathcal{L}_{FAR} . Notice that $\mathcal{L}_i^{1/\alpha}$ can have numerical issue when $\alpha \rightarrow 0, \mathcal{L}_i > 1$ or $\alpha \rightarrow +\infty, \mathcal{L}_i < 1$. The former case can cause computation overflow on forward propagation and the later case can cause computation overflow on backward propagation. Denote $\mathcal{L}_{\max} = \arg \max_{i=1}^M \mathcal{L}_i$ and $\mathcal{L}_{\min} = \arg \min_{i=1}^M \mathcal{L}_i$. We utilize the constant value of \mathcal{L}_{\max} or \mathcal{L}_{\min} to control $\mathcal{L}_{\text{FAR}}^{\text{KL}}$. It is easy to show $\mathcal{L}_{\text{FAR}}^{\text{KL}}$ has the following equivalent empirical formulation:

$$\mathcal{L}_{\text{FAR}}^{\text{KL}} = \begin{cases} \alpha \log \left(\frac{1}{M} \sum_{i=1}^M \left(\frac{\mathcal{L}_i}{\mathcal{L}_{\max}} \right)^{1/\alpha} \right) + \log \mathcal{L}_{\max}, & \alpha < 1. \\ \alpha \log \left(\frac{1}{M} \sum_{i=1}^M \left(\frac{\mathcal{L}_i}{\mathcal{L}_{\min}} \right)^{1/\alpha} \right) + \log \mathcal{L}_{\min}, & \alpha \geq 1. \end{cases} \quad (13)$$

by which we can avoid the numerical issue for both forward and backward propagation. In the remaining content of this work, we focus on balancing $\mathcal{L}_c^{\text{MAE}}$, $\mathcal{L}_{\text{diff}}^{\text{MSE}}$, $\mathcal{L}_{\text{diffnorm}}^{p=2}$ for FAR. We could potentially take $\mathcal{L}_c^{\text{MSE}}$ as the conventional regression loss, but we prefer a conventional regression loss that contains less derivative component (as shown in E.q. 6, MSE contains a fixed amount of derivative component). We present algorithm pseudocode in Alg.1.

Algorithm 1 Function Aligned Regression (FAR)

Require: hyper-parameter α for balancing sub-losses, training dataset $D = \{(\mathbf{x}_i, y_i)_{i=1}^N\}$.
 Initialize model $f(\cdot)$.
for $t = 1$ to T **do**
 Sample mini-batch of data $\{(\mathbf{x}_i, y_i)_{i \in B_t}\}$.
 Compute MAE loss $\mathcal{L}_c^{\text{MAE}}$.
 Compute the losses for derivative: $\mathcal{L}_{\text{diff}}^{\text{MSE}}$ and $\mathcal{L}_{\text{diffnorm}}^{p=2}$ by E.q. 7 and E.q. 9.
 Compute FAR (KL) loss $\mathcal{L}_{\text{FAR}}^{\text{KL}}$ by E.q. 13.
 Utilize SGD or Adam optimizers to optimize model with gradient $\nabla_f \mathcal{L}_{\text{FAR}}^{\text{KL}}$.
end for

Remark: the computational complexity for Alg.1 is $O(TB)$, where T is iteration number and B is batch size.

4. Experiments

In this section, we demonstrate the effectiveness of FAR with 2 synthetic datasets, 8 experimental settings with 5 tabular benchmark datasets and 1 image benchmark datasets. Further analysis for hyper-parameter α and running time of FAR are presented afterwards.

4.1 Synthetic Experiments

As most of the regression losses only explicitly focus on fitting the functional value, we utilize the two synthetic datasets to demonstrate the effectiveness of the proposed FAR for capturing both functional value and derivative value for the underlying ground truth in this subsection.

Datasets: 1) Sine: we take x_i from $[-10\pi, 10\pi]$ with the interval as 0.1 and $y_i = \sin(x_i)$. The data ground truth is presented as the grey solid line in Fig 1. 2) Squared sine: we take \tilde{x}_i from -1024 to 1024 with the interval as 0.1, then calculate $x_i = \text{sign}(\tilde{x}_i)\sqrt{|\tilde{x}_i|}$, which increases density of data from the region far from the origin. Finally, denote $\overline{x_i^2}$ as the empirical mean value of x_i^2 , make $y_i = x_i^2 \sin(x_i) / \overline{x_i^2}$, which magnifies the target values that are far from origin. The data ground truth is presented as the grey solid line in Fig 2.

Baselines: we compare the proposed FAR with 4 approaches: MAE, MSE, RNC and an extra heuristic fused loss (named MAE-Pearson) that combines MAE with negative Pearson correlation coefficient linearly:

$$\mathcal{L}_{\text{MAE}-\rho} = \beta \mathcal{L}_c^{\text{MAE}} + (1 - \beta) \mathcal{L}_{\text{diffnorm}}^{p=2}$$

where recall that $\mathcal{L}_{\text{diffnorm}}^{p=2} = 1 - \rho(f, y)$, and β is dynamically adjusted as the constant value of $\rho(f, y)$ on each iteration. Intuitively, when the Pearson correlation coefficient is high, the model focuses more on the MAE loss; and vice versa. It is worth noting that FAR can be further adapted to Symbolic Regression (SR) settings. For example, FAR loss could be defined as fitness function for evolutionary algorithm based method or reward function for reinforcement learning based method (Cranmer, 2023; Petersen et al., 2019). However, given that this work focuses on **Numeric Regression** (NR) setting, it is unfair to directly compare the proposed FAR under NR setting with SR methods. Because SR methods have already put the ground truth functions in their ‘toolbox’ (search candidates); on the other hand, there is no prior knowledge for FAR or other compared methods under NR setting. To elaborate the previous point, we extensively employ a well-established SR method, PySR¹ on the synthetic experiments. We find PySR performs perfectly when trigonometric functions are included in the search space. However, it performs much worse when we exclude trigonometric functions. Results are presented in the Appendix B.6.

Experimental Settings: for both of the synthetic datasets, we uniformly randomly sample half of the data as the training dataset. We utilize a 7-layer simple Feed Forward Neural Network (FFNN) with 5 hidden layers where neuron number for each layer is set as 100. We utilize ELU function as the activation function (Clevert et al., 2015). The total training epochs are set as 300 and batch size is set as 128. The initial learning rate is tuned in $\{1e-1, 1e-2, 1e-3, 1e-4\}$ for Adam optimizer (Kingma and Ba, 2014), which is stage-wised decreasing by 10 folds at the end of the 100-th and 200-th epoch. The weight decay is tuned in $\{1e-3, 1e-4, 1e-5, 0\}$. RNC takes the first 100 epochs are pre-training and the remaining as fine-tuning with MAE loss; temperature for RNC is tuned in $\{1, 2, 4\}$. For each baseline, we run 5 trials independently with the following 5 seeds: $\{1, 2, 3, 4, 5\}$. We set the $\alpha = 0.5$ for FAR on all synthetic experiments.

Results: the results on sine dataset are summarized in Fig. 1 and the results on squared sine dataset are summarized in Fig. 2. Due to the limited space, we include MSE results in Appendix B.5 for it is similar with MAE. On both of the datasets, we can see there is a clear advantage for the proposed FAR over the conventional MSE/MAE loss. For sine dataset, FAR captures approximately 1 or 2 more peaks than MSE/MAE loss. For squared sine dataset, FAR can almost recover the pattern (both shape and magnitude) of the ground truth data; however, MSE/MAE loss is hard to capture the pattern of the ground truth except a part of peaks with the largest magnitude. Compared with $\mathcal{L}_{\text{MAE}-\rho}$, FAR also demonstrate arguable advantages on both of the synthetic datasets, where FAR can capture more peaks on the sine dataset and captures magnitudes better on the squared sine dataset. FAR also outperforms RNC on both datasets.

4.2 Benchmark Experiments

We conduct experiments for FAR with other 8 competitive baselines on 6 real-world benchmark datasets with 8 extensive experimental tasks.

Baselines: the baselines for comparison are: 1) MAE. 2) MSE. 3) Huber loss (Huber, 1992). 4) Focal (MAE) (Yang et al., 2021): an variant for Focal loss with MAE loss, which put more learning weights on harder samples. 5) Focal (MSE) (Yang et al., 2021): combine

1. <https://astroautomata.com/PySR/>

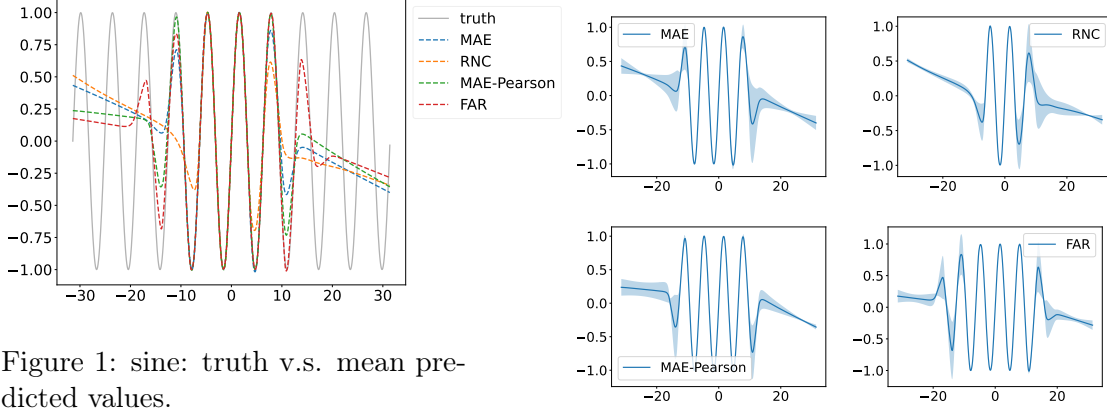


Figure 1: sine: truth v.s. mean predicted values.

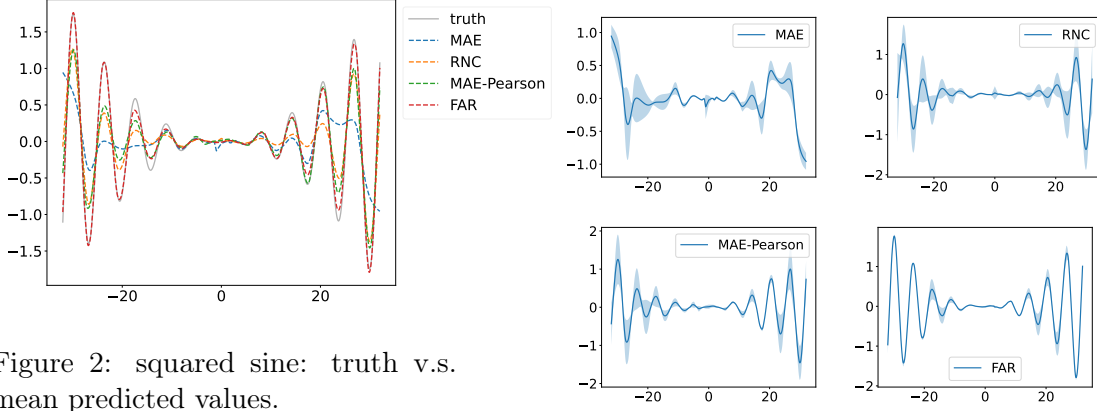


Figure 2: squared sine: truth v.s. mean predicted values.

Focal loss with MSE loss similarly as Focal (MAE). 6) RankSim (Gong et al., 2022): a regression method that regularizes predictions to maintain similar order with the their labels. 7) RNC (Zha et al., 2023): a state-of-the-art (SOTA) pre-training method for regression that enhances the prior that the pairwise similarities from learned latent features should be close to pairwise similarities from data labels. The method is based on a fashion of contrastive learning. 8) ConR (Keramati et al., 2023): a contrastive learning based SOTA regression method that combines conventional regression loss with a contrastive loss that pushes data latent features to be closer if their labels are closer. 9) FAR: the proposed Function Aligned regression loss that robustly reconciles: i) conventional regression loss on functional value; ii) regression loss on functional derivative; iii) regression loss on normalized functional derivative.

Datasets and Tasks: we conduct experiments with 8 extensive experimental settings on 6 real-world datasets: 1) Wine Quality (Cortez et al., 2009): predict wine quality based on physicochemical test values (such as acidity, sugar, chlorides, etc). 2) Abalone (Nash et al., 1995): predict the age of abalone from physical measurements (such as length, diameter, height, etc). 3) Parkinson (Total) (Tsanas et al., 2009): predict clinician’s total unified Parkinson’s disease rating scale (UPDRS) score by biomedical voice measurements from 42 people with early-stage Parkinson’s disease recruited to a six-month trial of a telemonitoring device for remote symptom progression monitoring. 4) Parkinson (Motor) (Tsanas et al., 2009): predict clinician’s motor UPDRS score with the same previous data feature. 5) Super

Table 1: Testing performance on the tabular datasets. Mean and standard deviation are reported. ‘Gains’ includes the percentages that FAR outperform the MAE and the best competitor (in parenthesis). The ‘p-values’ are calculated based on Student’s t-test for the ‘Gains’. p-value < 0.05 usually means significant difference. ↓ means the smaller the better; ↑ means the larger the better.

Dataset	Method	MAE	MSE	Huber	Focal (MAE)	Focal (MSE)	RankSim	RNC	ConR	FAR (ours)	Gains (%)	p-values
Wine Quality	MAE ↓	0.628(0.003)	0.625(0.004)	0.615(0.006)	0.624(0.011)	0.629(0.005)	0.627(0.006)	0.631(0.003)	0.63(0.007)	0.596(0.002)	5.13(3.14)	0.0(0.0)
	RMSE ↓	0.814(0.018)	0.807(0.006)	0.786(0.01)	0.791(0.011)	0.809(0.012)	0.796(0.011)	0.833(0.017)	0.798(0.01)	0.756(0.005)	7.13(3.83)	0.0(0.0)
	Pearson ↑	0.366(0.04)	0.442(0.02)	0.459(0.006)	0.446(0.012)	0.423(0.037)	0.427(0.036)	0.388(0.079)	0.412(0.032)	0.503(0.007)	37.37(9.6)	0.0(0.0)
	Spearman ↑	0.426(0.023)	0.454(0.013)	0.471(0.006)	0.458(0.013)	0.439(0.029)	0.44(0.03)	0.415(0.05)	0.43(0.028)	0.511(0.009)	20.0(8.65)	0.0(0.0)
Abalone	MAE ↓	1.503(0.013)	1.492(0.016)	1.501(0.013)	1.496(0.014)	1.497(0.008)	1.679(0.056)	1.647(0.079)	1.484(0.013)	1.494(0.016)	0.57(-0.72)	0.42(0.33)
	RMSE ↓	2.186(0.023)	2.159(0.039)	2.189(0.02)	2.174(0.029)	2.153(0.011)	2.511(0.099)	2.426(0.134)	2.197(0.028)	2.147(0.014)	1.61(0.29)	0.02(0.49)
	Pearson ↑	0.736(0.007)	0.737(0.011)	0.737(0.007)	0.739(0.004)	0.745(0.008)	0.665(0.045)	0.682(0.049)	0.736(0.006)	0.748(0.003)	1.81(0.49)	0.01(0.4)
	Spearman ↑	0.77(0.006)	0.776(0.001)	0.772(0.003)	0.771(0.001)	0.773(0.009)	0.735(0.014)	0.723(0.04)	0.772(0.002)	0.778(0.004)	1.03(0.27)	0.06(0.38)
Parkinson (Total)	MAE ↓	2.875(0.862)	3.464(0.029)	2.442(0.379)	2.693(0.91)	3.481(0.042)	8.616(0.007)	2.948(0.079)	3.581(0.519)	2.64(0.071)	8.15(-8.14)	0.6(0.33)
	RMSE ↓	4.803(0.809)	5.175(0.149)	4.498(0.392)	4.744(0.82)	5.157(0.14)	10.787(0.022)	4.786(0.103)	5.431(0.359)	4.258(0.206)	11.36(5.33)	0.23(0.31)
	Pearson ↑	0.891(0.038)	0.876(0.008)	0.909(0.017)	0.894(0.038)	0.877(0.007)	0.125(0.042)	0.896(0.004)	0.862(0.019)	0.922(0.009)	3.44(1.44)	0.15(0.21)
	Spearman ↑	0.87(0.047)	0.856(0.008)	0.895(0.02)	0.874(0.047)	0.855(0.006)	0.141(0.051)	0.876(0.002)	0.842(0.025)	0.907(0.01)	4.24(1.36)	0.16(0.31)
Parkinson (Motor)	MAE ↓	1.846(0.494)	2.867(0.092)	1.903(0.282)	1.599(0.047)	2.86(0.081)	6.891(0.013)	2.299(0.068)	2.698(0.466)	1.652(0.069)	10.52(-3.3)	0.46(0.24)
	RMSE ↓	3.336(0.491)	4.06(0.067)	3.226(0.35)	2.992(0.105)	4.083(0.116)	8.082(0.019)	3.632(0.136)	4.193(0.331)	2.68(0.134)	19.68(10.45)	0.03(0.01)
	Pearson ↑	0.91(0.029)	0.865(0.005)	0.917(0.019)	0.93(0.005)	0.863(0.008)	0.125(0.043)	0.894(0.008)	0.854(0.023)	0.943(0.006)	3.71(1.48)	0.05(0.01)
	Spearman ↑	0.902(0.032)	0.854(0.004)	0.912(0.019)	0.924(0.006)	0.854(0.009)	0.144(0.036)	0.885(0.008)	0.843(0.024)	0.939(0.006)	4.16(1.63)	0.05(0.01)
Super Conductivity	MAE ↓	8.365(0.027)	7.717(0.014)	7.42(0.052)	8.351(0.025)	7.713(0.007)	11.99(0.403)	6.238(0.078)	8.368(0.022)	6.257(0.027)	25.2(-0.31)	0.0(0.05)
	RMSE ↓	13.677(0.061)	12.158(0.113)	12.639(0.067)	13.631(0.039)	12.13(0.107)	17.089(0.408)	11.106(0.18)	13.68(0.084)	10.745(0.183)	21.44(3.25)	0.0(0.02)
	Pearson ↑	0.918(0.0)	0.935(0.001)	0.93(0.001)	0.918(0.0)	0.935(0.001)	0.867(0.007)	0.947(0.001)	0.918(0.001)	0.949(0.002)	3.39(0.24)	0.0(0.06)
	Spearman ↑	0.915(0.001)	0.924(0.0)	0.93(0.001)	0.916(0.001)	0.925(0.0)	0.86(0.008)	0.943(0.001)	0.917(0.001)	0.944(0.002)	3.13(0.15)	0.0(0.18)
IC50	MAE ↓	1.364(0.002)	1.382(0.004)	1.366(0.004)	1.365(0.001)	1.386(0.01)	1.384(0.009)	2.143(0.242)	1.34(0.025)	1.359(0.003)	0.37(-1.43)	0.02(0.16)
	RMSE ↓	1.706(0.013)	1.699(0.008)	1.702(0.002)	1.696(0.003)	1.707(0.014)	1.809(0.13)	2.454(0.235)	1.668(0.022)	1.7(0.005)	0.39(-1.89)	0.38(0.02)
	Pearson ↑	0.085(0.049)	0.021(0.013)	0.069(0.061)	0.104(0.029)	0.023(0.017)	0.012(0.026)	0.018(0.05)	0.202(0.033)	0.302(0.028)	252.97(49.13)	0.0(0.0)
	Spearman ↑	0.114(0.032)	0.065(0.039)	0.087(0.054)	0.109(0.033)	0.064(0.04)	0.033(0.028)	0.038(0.05)	0.184(0.04)	0.26(0.024)	127.64(40.86)	0.0(0.01)
AgeDB (Scratch)	MAE ↓	6.449(0.058)	6.517(0.097)	6.387(0.046)	6.404(0.037)	6.567(0.107)	6.502(0.085)	—	6.43(0.028)	6.286(0.034)	2.52(1.58)	0.0(0.01)
	RMSE ↓	8.509(0.078)	8.608(0.046)	8.418(0.045)	8.476(0.067)	8.617(0.104)	8.596(0.188)	—	8.49(0.049)	8.268(0.05)	2.83(1.79)	0.0(0.0)
	Pearson ↑	0.917(0.002)	0.914(0.001)	0.918(0.001)	0.918(0.002)	0.914(0.001)	0.916(0.005)	—	0.916(0.002)	0.921(0.001)	0.48(0.35)	0.0(0.0)
	Spearman ↑	0.919(0.002)	0.917(0.001)	0.92(0.0)	0.92(0.002)	0.916(0.001)	0.918(0.004)	—	0.919(0.003)	0.923(0.002)	0.41(0.28)	0.01(0.01)
AgeDB (RNC Linear Probe)	R ² ↑	0.836(0.003)	0.833(0.002)	0.84(0.002)	0.838(0.003)	0.832(0.004)	0.833(0.007)	—	0.837(0.002)	0.846(0.002)	1.15(0.67)	0.0(0.0)
	MAE ↓	6.124(0.039)	6.13(0.058)	6.124(0.086)	6.102(0.039)	6.139(0.033)	—	—	—	6.069(0.022)	0.89(0.55)	0.04(0.17)
	RMSE ↓	8.077(0.036)	8.099(0.04)	8.108(0.068)	8.073(0.029)	8.113(0.037)	—	—	—	8.054(0.014)	0.28(0.23)	0.28(0.29)
	Pearson ↑	0.924(0.0)	0.924(0.0)	0.924(0.0)	0.924(0.0)	0.924(0.0)	—	—	—	0.924(0.0)	0.0(0.0)	1.0(1.0)
RNC Linear Probe	Spearman ↑	0.927(0.0)	0.927(0.0)	0.927(0.0)	0.927(0.0)	0.926(0.0)	—	—	—	0.927(0.0)	0.0(0.0)	1.0(1.0)
	R ² ↑	0.853(0.001)	0.852(0.002)	0.852(0.003)	0.853(0.001)	0.851(0.001)	—	—	—	0.854(0.0)	0.12(0.07)	0.2(0.35)

Conductivity (Hamidieh, 2018): predict the critical temperature for super conductors with 81 extracted material features. 6) IC50 (Garnett et al., 2012): predict drugs’ half-maximal inhibitory concentration (IC50) for 15 drugs filtered from 130 total drugs with missing-value-control over 639 human tumour cell lines. We include more details about data preprocessing in the appendix. 7) AgeDB (Scratch) (Moschoglou et al., 2017): predict age from face images. All baselines are trained from scratch. 8) AgeDB (RNC Linear Probe) (Moschoglou et al., 2017): predict age with the latent features from a pre-trained RNC model (Zha et al., 2023). The statistics of the datasets are summarized in Table 3 in Appendix B.1.

Models: for the tabular datasets (Abalone and Wine Quality) with feature dimension less equal to 16, we utilize a 6-layer-FFNN with hidden neurons as (16, 32, 16, 8) as the backbone model. For the tabular datasets (Parkinson (Total), Parkinson (Motor) and Super Conductivity) with feature dimension larger to 16 and less equal to 128, we utilize a 6-layer-FFNN with hidden neurons as (128, 256, 128, 64) as the backbone model; we employ the same (128, 256, 128, 64) FFNN model for IC50 except generating 15 linear heads for predicting the 15 targets. All FFNN variants utilize ELU as the activation in this work. For AgeDB (Scratch), we follow the previous work and employ ResNet18 as the backbone model (Zha et al., 2023). For AgeDB (RNC Linear Probe), we simply apply linear model based on the latent feature pre-trained with RNC.

Experimental Settings: for tabular datasets, we uniformly randomly split 20% data as testing; the remaining 80% as training and validation, where we conduct 5-fold-cross-validation with random seed set as 123. The total training epochs is set as 100 and batch size is set as 256. The weight decay for each method is tuned in {1e-3, 1e-4, 1e-5}; we utilize

SGD with momentum (set as 0.9) optimizer and tune the initial learning rate for baseline method in $\{1e-1, 1e-2, 1e-3, 1e-4, 1e-5\}$, which is stage-wised decreased by 10 folds at the end of 50-th and 75-th epoch. The switching hyper-parameter δ for Huber loss and the scaling hyper-parameter β for Focal (MAE) or Focal (MSE) loss are tuned in $\{0.25, 1, 4\}$. The interpolation hyper-parameter λ for RankSim is tuned in $\{0.5, 1, 2\}$ and the balancing hyper-parameter γ is fixed as 100 as suggested by their sensitivity study in their Appendix C.4 (Gong et al., 2022). The temperature hyper-parameter for RNC is tuned in $\{1, 2, 4\}$; the first 50 epochs are used for RNC pre-training and the remaining 50 epochs are used for fine-tuning with MAE loss. The linear combination hyper-parameters α is fixed as 1, β is tuned in $\{0.2, 1, 4\}$ for ConR, as suggested by the ablation study in their Appendix A.5 (Keramati et al., 2023). The robust reconciliation hyper-parameter α for FAR is tuned in $\{0.1, 1, 10\}$. The model performance is evaluated with the following 4 metrics: MAE, RMSE, Pearson correlation coefficient, Spearman’s rank correlation coefficient. The best testing performance for each baseline method on each training fold is decided by its best validation performance on the same training fold over (initial learning rate, weight decay, method-special-hyper-parameter, the epoch for evaluation) combinations. For IC50 with 15 targets, we report the averaged value across all targets. For AgeDB dataset, we follow the same setting for RNC linear probe task and similar setting for training from scratch task. We include the complete details in Appendix B.3. Because RNC is a pre-training method, it doesn’t have evaluation on training from scratch task. Instead, all baselines in linear probe are based on RNC pre-trained latent features. Because RankSim and ConR are proposed to manipulate latent feature, they don’t have evaluation on linear probe task where the trainable model is linear. We additionally include Coefficient of determination (R^2) as an evaluation metric for AgeDB besides of the previous 4 evaluation metrics.

Results: all the testing results are summarized in Table 1. The proposed FAR outperform all the competitors from the perspective of Pearson Correlation Coefficient and Spearman’s Correlation Coefficient over all the experimental settings. It is possibly due to these two metrics measures the functional shape (derivatives) alignment of prediction v.s. ground truth, which is explicitly captured by FAR. FAR also outperform most of the competitors from perspective of RMSE, except IC50. It is reasonable because MSE can be decoupled as local derivative components and global deviation component, as shown in E.q. 6. For MAE evaluations, although FAR is not always the best, it is not significant worse than the best competitor. Besides, FAR outperform MAE for all metrics evaluations (except the ties), which demonstrates the functional derivative components improve the vanilla MAE. Finally, FAR achieves new SOTA results on AgeDB for both training from scratch and linear probe settings with ResNet18. For scratch setting, FAR achieves 6.286(0.034) for MAE and 0.846(0.002) for R^2 score, while the previous SOTA is 6.40 for MAE and 0.830 for R^2 score; for 2-stage linear probe on RNC pre-trained feature setting, FAR achieves 6.069(0.022) for MAE and 0.854(0.0) for R^2 score, while the previous SOTA is 6.14 for MAE and 0.850 for R^2 score (Zha et al., 2023).

4.3 Further Analysis

We additionally provide sensitivity analysis on robust reconciliation hyper-parameter α for FAR and practical training efficiency comparison in this subsection.

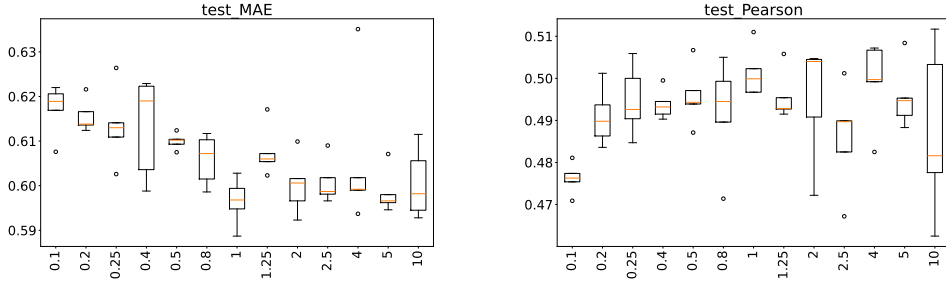


Figure 3: Different α (x-axis) for FAR on Wine Quality.

Sensitivity on α : we conduct extensive hyper-parameter search for α in $\{0.1, 0.2, 0.25, 0.4, 0.5, 0.8, 1, 1.25, 2, 2.5, 4, 5, 10\}$. The initial learning rate and weight decay are still searched in the same sets as previously described. We include the partial results on Wine Quality in Table 3 and full results are included in Appendix B.2. As observed from the box-plot, FAR is not very sensitive to α but it is still suggested to tune it in the $[0.1, 10]$ range.

Table 2: Running time (seconds/epoch) on 3 benchmark datasets. Repeated 1500 epochs, mean and standard deviation are reported.

Dataset	Wine Quality	Abalone	Super Conductivity
MAE	0.102(0.007)	0.09(0.005)	0.934(0.073)
MSE	0.102(0.006)	0.091(0.006)	0.918(0.072)
Huber	0.101(0.006)	0.09(0.005)	0.941(0.074)
Focal (MAE)	0.103(0.007)	0.092(0.006)	0.958(0.072)
Focal (MSE)	0.103(0.006)	0.092(0.006)	0.935(0.073)
RankSim	0.116(0.007)	0.111(0.006)	6.89(0.073)
RNC	0.674(0.04)	0.396(0.025)	7.95(0.189)
ConR	0.129(0.006)	0.106(0.006)	1.213(0.071)
FAR (ours)	0.098(0.005)	0.089(0.005)	0.96(0.072)

Training Efficiency: we practically run all baselines sequentially on a cluster node with AMD EPYC 7402 24-Core Processor 2.0 GHz. Each baseline runs 1500 epochs on Wine Quality, Abalone, Super Conductivity datasets. The results are summarized in Table 2 in appendix. From the observation, we find FAR is as efficient as the most efficient conventional regression loss, such as MAE, MSE, etc. It is consistent with the theoretical analysis that FAR only takes $O(TB)$ complexity. On the other hand, the pairwise latent feature based regression methods, such as RankSim, ConR and RNC, are clearly slower than FAR.

5. Conclusion

In this work, we discover the caveat that the conventional regression loss functions only focus on learning the functional values from the data, which could be sub-optimal for learning the functional derivatives of the ground truth. Motivated by this, we propose to explicitly learn the functional derivatives from the data, that is, Function Aligned Regression (FAR). With mathematical transformations, we convert the pairwise derivative loss to the efficient linear

form. Furthermore, we propose a robust reconciliation approach for FAR that trade-off the different sub-losses with different magnitudes. The effectiveness of the proposed FAR method has been practically demonstrated on 2 synthetic datasets and 8 experimental settings across 6 benchmark datasets.

Acknowledgments

This research was partially funded by NIH U01HG012069 and Allen Distinguished Investigator Award, a Paul G. Allen Frontiers Group advised grant of the Paul G. Allen Family Foundation.

Appendix A. Proofs

A.1 Proof for Corollary 1

Proof

$f(\mathbf{x}_1) - f(\mathbf{x}_2) = \mathcal{Y}(\mathbf{x}_1) - \mathcal{Y}(\mathbf{x}_2), \forall (\mathbf{x}_1, \mathcal{Y}(\mathbf{x}_1)), (\mathbf{x}_2, \mathcal{Y}(\mathbf{x}_2)) \in \mathcal{D} \implies \nabla^k f(\mathbf{x}) = \nabla^k \mathcal{Y}(\mathbf{x}), \forall (\mathbf{x}, \mathcal{Y}(\mathbf{x})) \in \mathcal{D}, k = \{1, 2, \dots\}$

First, we prove that $\nabla f(\mathbf{x}) = \nabla \mathcal{Y}(\mathbf{x}), \forall (\mathbf{x}, \mathcal{Y}(\mathbf{x})) \in \mathcal{D}$.

Take two neighbors $\mathbf{x}_1, \mathbf{x}_2$ that are infinitely close to an arbitrary \mathbf{x} . By mean value theorem for multiple variables (Rudin et al., 1976): $f(\mathbf{x}_1) - f(\mathbf{x}_2) = \nabla f(\xi)^\top (\mathbf{x}_1 - \mathbf{x}_2), \mathcal{Y}(\mathbf{x}_1) - \mathcal{Y}(\mathbf{x}_2) = \nabla \mathcal{Y}(\gamma)^\top (\mathbf{x}_1 - \mathbf{x}_2)$, where ξ, γ are two points that are infinitely close to \mathbf{x} . Because $f(\mathbf{x}_1) - f(\mathbf{x}_2) = \mathcal{Y}(\mathbf{x}_1) - \mathcal{Y}(\mathbf{x}_2), \forall (\mathbf{x}_1, \mathcal{Y}(\mathbf{x}_1)), (\mathbf{x}_2, \mathcal{Y}(\mathbf{x}_2)) \in \mathcal{D}$, we have $\nabla f(\xi)^\top (\mathbf{x}_1 - \mathbf{x}_2) = \nabla \mathcal{Y}(\gamma)^\top (\mathbf{x}_1 - \mathbf{x}_2)$.

As $\mathbf{x}_1, \mathbf{x}_2$ are infinitely close, ξ, γ collapse to the same point \mathbf{x} . Therefore, $\nabla f(\mathbf{x}) = \nabla \mathcal{Y}(\mathbf{x})$.

Next, we show $\nabla^k f(\mathbf{x}) = \nabla^k \mathcal{Y}(\mathbf{x}), \forall (\mathbf{x}, \mathcal{Y}(\mathbf{x})) \in \mathcal{D}, k = \{2, \dots\}$ by induction. Assume we have $\nabla^k f(\mathbf{x}) = \nabla^k \mathcal{Y}(\mathbf{x}), \forall (\mathbf{x}, \mathcal{Y}(\mathbf{x})) \in \mathcal{D}$, to show $\nabla^{k+1} f(\mathbf{x}) = \nabla^{k+1} \mathcal{Y}(\mathbf{x}), \forall (\mathbf{x}, \mathcal{Y}(\mathbf{x})) \in \mathcal{D}$.

Denote i -th element from $\nabla^k f(\mathbf{x})$ as $[\nabla^k f(\mathbf{x})]_i$. Take two neighbors $\mathbf{x}_1, \mathbf{x}_2$ that are infinitely close to arbitrary \mathbf{x} and apply mean value theorem for multiple variables solely on the i -th element: $[\nabla^k f(\mathbf{x}_1)]_i - [\nabla^k f(\mathbf{x}_2)]_i = \nabla_i^{k+1} f(\xi_i)(\mathbf{x}_1 - \mathbf{x}_2), [\nabla^k \mathcal{Y}(\mathbf{x}_1)]_i - [\nabla^k \mathcal{Y}(\mathbf{x}_2)]_i = \nabla_i^{k+1} \mathcal{Y}(\gamma_i)(\mathbf{x}_1 - \mathbf{x}_2)$, where $\nabla_i^{k+1} f(\xi_i)$ represents the higher order gradient taken for $[\nabla^k f(\mathbf{x})]_i$ regarding to variables. It is worth noting that ξ_i can be different points for different i , which hamper the general mean value theorem for vector-valued functions in the literature (Rudin et al., 1976) but doesn't harm the specific proof here. Similarly, because $[\nabla^k f(\mathbf{x}_1)]_i - [\nabla^k f(\mathbf{x}_2)]_i = [\nabla^k \mathcal{Y}(\mathbf{x}_1)]_i - [\nabla^k \mathcal{Y}(\mathbf{x}_2)]_i, \forall \mathbf{x}_1, \mathbf{x}_2$, we have $\nabla_i^{k+1} f(\xi_i)(\mathbf{x}_1 - \mathbf{x}_2) = \nabla_i^{k+1} \mathcal{Y}(\gamma_i)(\mathbf{x}_1 - \mathbf{x}_2)$.

As $\mathbf{x}_1, \mathbf{x}_2$ are infinitely close, ξ_i, γ_i collapse to the same point $\mathbf{x}, \forall i$. Therefore, $\nabla_i^{k+1} f(\mathbf{x}) = \nabla_i^{k+1} \mathcal{Y}(\mathbf{x}), \forall i$; thereby $\nabla^{k+1} f(\mathbf{x}) = \nabla^{k+1} \mathcal{Y}(\mathbf{x})$.

Next, we prove the other direction.

$\nabla^k f(\mathbf{x}) = \nabla^k \mathcal{Y}(\mathbf{x}), \forall (\mathbf{x}, \mathcal{Y}(\mathbf{x})) \in \mathcal{D}, k = \{1, 2, \dots\} \implies f(\mathbf{x}_1) - f(\mathbf{x}_2) = \mathcal{Y}(\mathbf{x}_1) - \mathcal{Y}(\mathbf{x}_2), \forall (\mathbf{x}_1, \mathcal{Y}(\mathbf{x}_1)), (\mathbf{x}_2, \mathcal{Y}(\mathbf{x}_2)) \in \mathcal{D}$

$\nabla^k f(\mathbf{x}) = \nabla^k \mathcal{Y}(\mathbf{x}), \forall (\mathbf{x}, \mathcal{Y}(\mathbf{x})) \in \mathcal{D} \implies \nabla f(\mathbf{x}) = \nabla \mathcal{Y}(\mathbf{x}), \forall (\mathbf{x}, \mathcal{Y}(\mathbf{x})) \in \mathcal{D}$. We take infinitely small but infinitely many steps $\epsilon_i, i = 1, \dots, \infty$ that constitute a path from \mathbf{x}_1 to \mathbf{x}_2 . By mean value theorem for multiple variables, $f(\mathbf{x}_1 + \sum_{i=1}^k \epsilon_i) - f(\mathbf{x}_1 + \sum_{i=1}^{k-1} \epsilon_i) = \nabla f(\mathbf{x}_1 + \sum_{i=1}^k \epsilon_i)^\top (\epsilon_k), \mathcal{Y}(\mathbf{x}_1 + \sum_{i=1}^k \epsilon_i) - \mathcal{Y}(\mathbf{x}_1 + \sum_{i=1}^{k-1} \epsilon_i) = \nabla \mathcal{Y}(\mathbf{x}_1 + \sum_{i=1}^k \epsilon_i)^\top (\epsilon_k)$.

Therefore, $\sum_{k=1}^\infty f(\mathbf{x}_1 + \sum_{i=1}^k \epsilon_i) - f(\mathbf{x}_1 + \sum_{i=1}^{k-1} \epsilon_i) = \sum_{k=1}^\infty \mathcal{Y}(\mathbf{x}_1 + \sum_{i=1}^k \epsilon_i) - \mathcal{Y}(\mathbf{x}_1 + \sum_{i=1}^{k-1} \epsilon_i)$; and by telescoping sum, $f(\mathbf{x}_2) - f(\mathbf{x}_1) = \mathcal{Y}(\mathbf{x}_2) - \mathcal{Y}(\mathbf{x}_1)$. ■

A.2 Proof for Corollary 2

Proof Basically directly switching the order by definition.

$$\begin{aligned}
\mathcal{L}_{\text{diff}}^p &= \frac{1}{N^2} \sum_{i=1}^N \sum_{j=1}^N \ell(f(\mathbf{x}_i) - f(\mathbf{x}_j), \mathcal{Y}(\mathbf{x}_i) - \mathcal{Y}(\mathbf{x}_j)) \\
&= \frac{1}{N^2} \sum_{i=1}^N \sum_{j=1}^N [f(\mathbf{x}_i) - f(\mathbf{x}_j) - (\mathcal{Y}(\mathbf{x}_i) - \mathcal{Y}(\mathbf{x}_j))]^p \\
&= \frac{1}{N^2} \sum_{i=1}^N \sum_{j=1}^N [f(\mathbf{x}_i) - \mathcal{Y}(\mathbf{x}_i) - (f(\mathbf{x}_j) - \mathcal{Y}(\mathbf{x}_j))]^p \\
&= \frac{1}{N^2} \sum_{i=1}^N \sum_{j=1}^N \ell(\sigma_{\mathbf{x}_i}^f, \sigma_{\mathbf{x}_j}^f)
\end{aligned}$$

■

A.3 Proof for Theorem 3

Proof

Recall that $\bar{\sigma}_{\mathbf{x}}^f = \frac{1}{N} \sum_{i=1}^N \sigma_{\mathbf{x}_i}^f$ denotes the empirical mean.

$$\begin{aligned}
\mathcal{L}_{\text{diff}}^{\text{MSE}} &= \frac{1}{N^2} \sum_{i=1}^N \sum_{j=1}^N \frac{1}{2} [f(\mathbf{x}_i) - \mathcal{Y}(\mathbf{x}_i) - (f(\mathbf{x}_j) - \mathcal{Y}(\mathbf{x}_j))]^2 \\
&= \frac{1}{2N^2} \sum_{i=1}^N \sum_{j=1}^N (\sigma_{\mathbf{x}_i}^f - \sigma_{\mathbf{x}_j}^f)^2 \\
&= \frac{1}{2N^2} \sum_{i=1}^N \sum_{j=1}^N (\sigma_{\mathbf{x}_i}^f - \bar{\sigma}_{\mathbf{x}}^f + \bar{\sigma}_{\mathbf{x}}^f - \sigma_{\mathbf{x}_j}^f)^2 \\
&= \frac{1}{N} \sum_{i=1}^N (\sigma_{\mathbf{x}_i}^f - \bar{\sigma}_{\mathbf{x}}^f)^2 \\
&= \text{Var}(\sigma_{\mathbf{x}}^f)
\end{aligned}$$

where the cross terms expanded out in the third equation can be canceled when iterate across all data samples.

■

A.4 Proof for Corollary 5

Proof Recall that $df_{i,j} = f(\mathbf{x}_i) - f(\mathbf{x}_j)$ and $d\mathcal{Y}_{i,j} = \mathcal{Y}(\mathbf{x}_i) - \mathcal{Y}(\mathbf{x}_j)$, and $\mathbf{df} = [df_{1,1}, df_{1,2}, \dots, df_{N,N-1}, df_{N,N}]$, $\mathbf{dY} = [d\mathcal{Y}_{1,1}, d\mathcal{Y}_{1,2}, \dots, d\mathcal{Y}_{N,N-1}, d\mathcal{Y}_{N,N}]$.

$$\begin{aligned}
 \mathcal{L}_{\text{diffnorm}}^{p=2} &= \left\| \frac{\mathbf{df}}{\|\mathbf{df}\|_2} - \frac{\mathbf{dY}}{\|\mathbf{dY}\|_2} \right\|_2^2 \\
 &\quad (\text{by Theorem 3}) \\
 &= \left\| \frac{\mathbf{df}}{\sqrt{2N^2 \text{Var}(f)}} - \frac{\mathbf{dY}}{\sqrt{2N^2 \text{Var}(y)}} \right\|_2^2 \\
 &= \frac{1}{2N^2} \sum_{i=1}^N \sum_{j=1}^N \left(\frac{f(\mathbf{x}_i) - f(\mathbf{x}_j)}{\text{Var}(f)} - \frac{\mathcal{Y}(\mathbf{x}_i) - \mathcal{Y}(\mathbf{x}_j)}{\text{Var}(y)} \right)^2 \\
 &= \frac{1}{2N^2} \sum_{i=1}^N \sum_{j=1}^N \left(\frac{f(\mathbf{x}_i) - \bar{f} + \bar{f} - f(\mathbf{x}_j)}{\text{Var}(f)} - \frac{\mathcal{Y}(\mathbf{x}_i) - \bar{y} + \bar{y} - \mathcal{Y}(\mathbf{x}_j)}{\text{Var}(y)} \right)^2 \\
 &\quad (\text{by algebras, there are } 2N \text{ repeats}) \\
 &= \frac{2N}{2N^2} \left[\sum_{i=1}^N \left(\frac{f(\mathbf{x}_i) - \bar{f}}{\text{Var}(f)} \right)^2 - 2 \left(\frac{f(\mathbf{x}_i) - \bar{f}}{\text{Var}(f)} \right) \left(\frac{\mathcal{Y}(\mathbf{x}_i) - \bar{y}}{\text{Var}(y)} \right) + \left(\frac{\mathcal{Y}(\mathbf{x}_i) - \bar{y}}{\text{Var}(y)} \right)^2 \right] \\
 &= \frac{1}{2N} \sum_{i=1}^N \left(\frac{(f(\mathbf{x}_i) - \bar{f})}{\sqrt{\text{Var}(f)}} - \frac{(y_i - \bar{y})}{\sqrt{\text{Var}(y)}} \right)^2 \\
 &= 1 - \frac{\text{Cov}(f, y)}{\sqrt{\text{Var}(f)\text{Var}(y)}} = 1 - \rho(f, y)
 \end{aligned}$$

■

A.5 Proof for Theorem 6

Proof

$$\mathcal{L}_{\text{FAR}}^{\text{KL}}(\mathcal{L}_1, \dots, \mathcal{L}_M; \alpha) = \max_{\mathbf{p} \in \Delta_M} \sum_{i=1}^M p_i \log \mathcal{L}_i - \alpha \text{KL}(\mathbf{p} | \frac{\mathbf{1}}{M})$$

By Lagrangian multiplier:

$$\mathcal{L}_{\text{FAR}}^{\text{KL}}(\mathcal{L}_1, \dots, \mathcal{L}_M; \alpha) = \max_{\mathbf{p}} \min_{\mathbf{a} \geq 0, b} \sum_{i=1}^M p_i \log \mathcal{L}_i - \alpha \text{KL}(\mathbf{p} | \frac{\mathbf{1}}{M}) + \sum_{i=1}^M a_i p_i - b \left(\sum_{i=1}^M p_i - 1 \right) \quad (14)$$

By stationary condition of \mathbf{p} :

$$p_i^* = \frac{1}{M} \exp \left(\frac{\log \mathcal{L}_i + a_i - b}{\alpha} - 1 \right)$$

Take the optimal \mathbf{p}^* back to E.q. 14:

$$\mathcal{L}_{\text{FAR}}^{\text{KL}}(\mathcal{L}_1, \dots, \mathcal{L}_M; \alpha) = \min_{\mathbf{a} \geq 0, b} b + \alpha \sum_{i=1}^M \frac{1}{M} \exp\left(\frac{\log \mathcal{L}_i + a_i - b}{\alpha} - 1\right) \quad (15)$$

a_i can be minimized as 0, $\forall i$, because $\alpha \geq 0$. Further take the stationary condition for b :

$$\begin{aligned} 1 &= \sum_{i=1}^M \frac{1}{M} \exp\left(\frac{\log \mathcal{L}_i - b^*}{\alpha} - 1\right) \\ \exp(b^*/\alpha) &= \sum_{i=1}^M \frac{1}{M} \exp\left(\frac{\log \mathcal{L}_i}{\alpha} - 1\right) \end{aligned}$$

Take the optimal solution b^* back to E.q. 15:

$$\begin{aligned} \mathcal{L}_{\text{FAR}}^{\text{KL}}(\mathcal{L}_1, \dots, \mathcal{L}_M; \alpha) &= \alpha \log \left[\sum_{i=1}^M \frac{1}{M} \exp\left(\frac{\log \mathcal{L}_i}{\alpha} - 1\right) \right] + \alpha \\ &= \alpha \log \sum_{i=1}^M \frac{1}{M} \exp\left(\frac{\log \mathcal{L}_i}{\alpha}\right) \\ &= \alpha \log \left(\frac{1}{M} \sum_{i=1}^M \mathcal{L}_i^{1/\alpha} \right) \end{aligned} \quad (16)$$

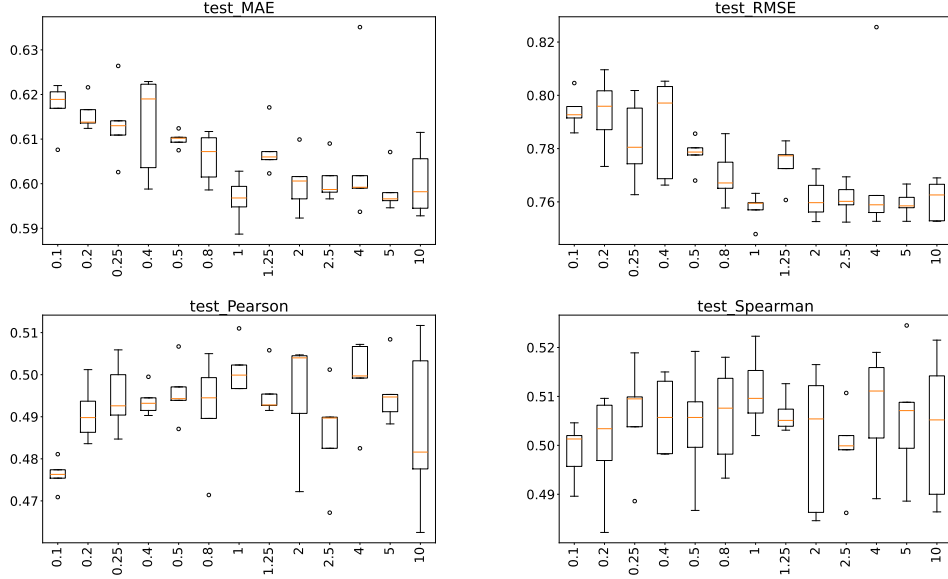
Therefore,

$$\exp(\mathcal{L}_{\text{FAR}}^{\text{KL}}(\mathcal{L}_1, \dots, \mathcal{L}_M; \alpha)) = \left(\frac{1}{M} \sum_{i=1}^M \mathcal{L}_i^{1/\alpha} \right)^\alpha$$

When $\alpha = 1$, we recover the Arithmetic Mean. Next we discuss the cases that $\alpha \rightarrow +\infty$ and $\alpha \rightarrow 0$. By L'Hôpital's rule:

$$\begin{aligned} \lim_{\alpha \rightarrow +\infty} \mathcal{L}_{\text{FAR}}^{\text{KL}}(\mathcal{L}_1, \dots, \mathcal{L}_M; \alpha) &= \lim_{\alpha \rightarrow +\infty} \frac{\log(\frac{1}{M} \sum_{i=1}^M \mathcal{L}_i^{1/\alpha})}{1/\alpha} \\ &= \lim_{\alpha \rightarrow +\infty} \frac{\sum_{i=1}^M \mathcal{L}_i^{1/\alpha} \log \mathcal{L}_i}{\mathcal{L}_i^{1/\alpha}} \\ &= \frac{\sum_{i=1}^M \log \mathcal{L}_i}{M} \end{aligned}$$

Hence, $\lim_{\alpha \rightarrow +\infty} \exp(\mathcal{L}_{\text{FAR}}^{\text{KL}}) = (\prod_{i=1}^M \mathcal{L}_i)^{\frac{1}{M}}$. By the same logic, $\lim_{\alpha \rightarrow 0} \exp(\mathcal{L}_{\text{FAR}}^{\text{KL}}) = \max_{i=1}^M \mathcal{L}_i$. ■


 Figure 4: Different α (x-axis) for FAR on Wine Quality.

Appendix B. More Experiments

B.1 Dataset Statistics

The statistics for benchmark datasets are summarized as following. The AgeDB is a image dataset where the image size is not identical. The # of feature is measured after data pre-processing.

Table 3: Dataset Statistics

Dataset	# of instance	# of feature	# of targets
Wine Quality	4898	11	1
Abalone	4177	10	1
Parkinson	5875	19	2
Super Conductivity	21263	81	1
IC50	429	966	15
AgeDB	16488	—	1

B.2 Sensitivity Analysis

We include the sensitivity results for FAR on Wine Quality, Abalone, Parkinson (Total), Parkinson (Motor), Super Conductivity as in Fig. 4,5,6,7,8. As we mentioned in the main content, the α is not very sensitive, but it is suggested to be tuned in $[0.1,10]$ region.

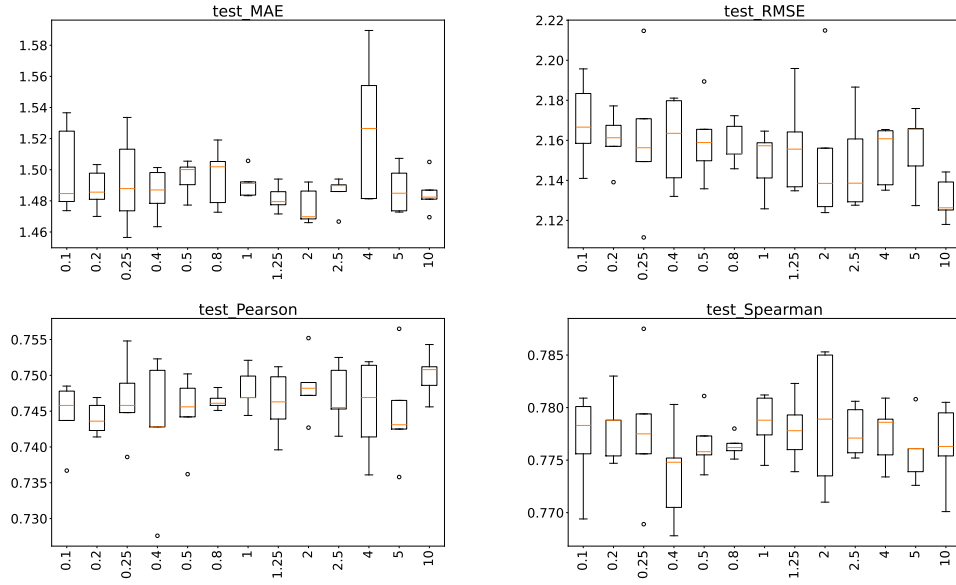


Figure 5: Different α (x-axis) for FAR on Abalone.

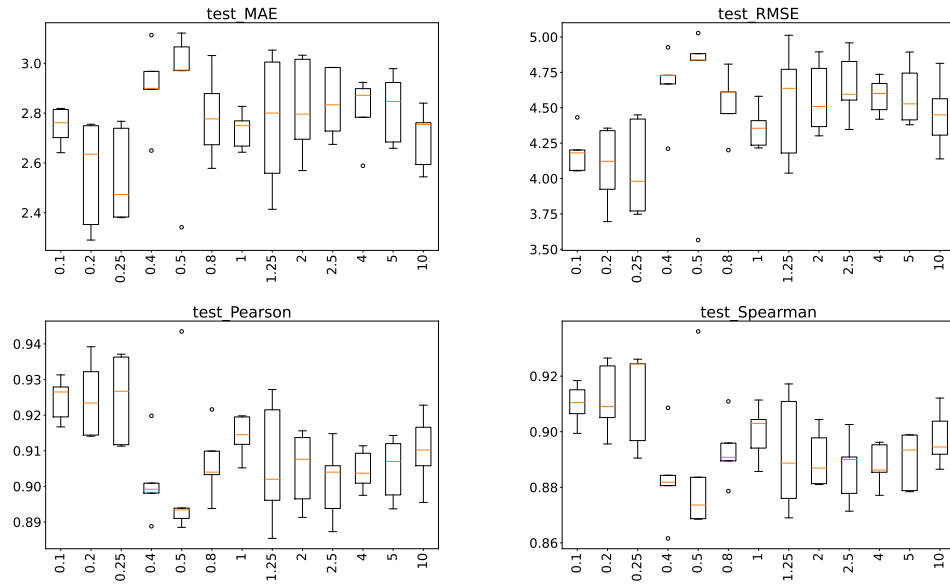


Figure 6: Different α (x-axis) for FAR on Parkinson (Total).

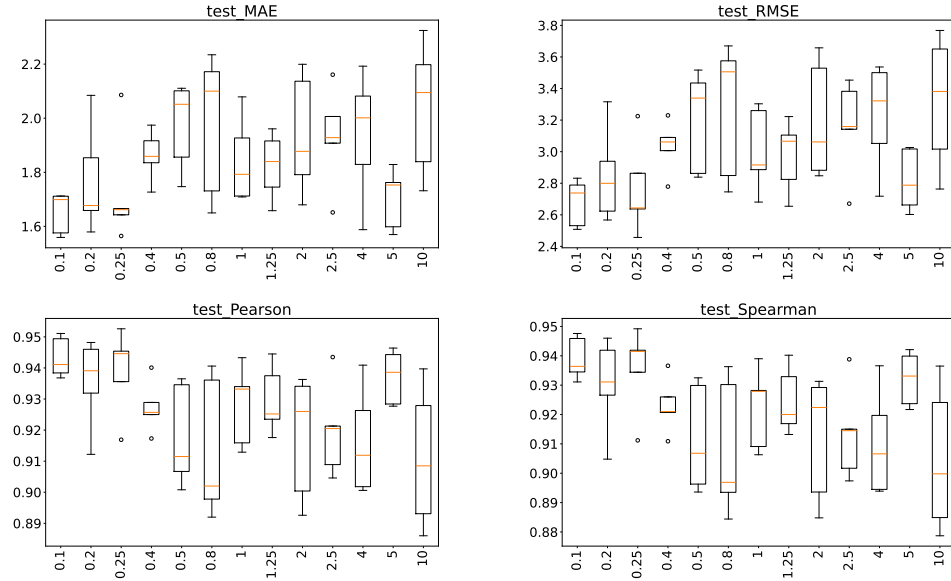


Figure 7: Different α (x-axis) for FAR on Parkinson (Motor).

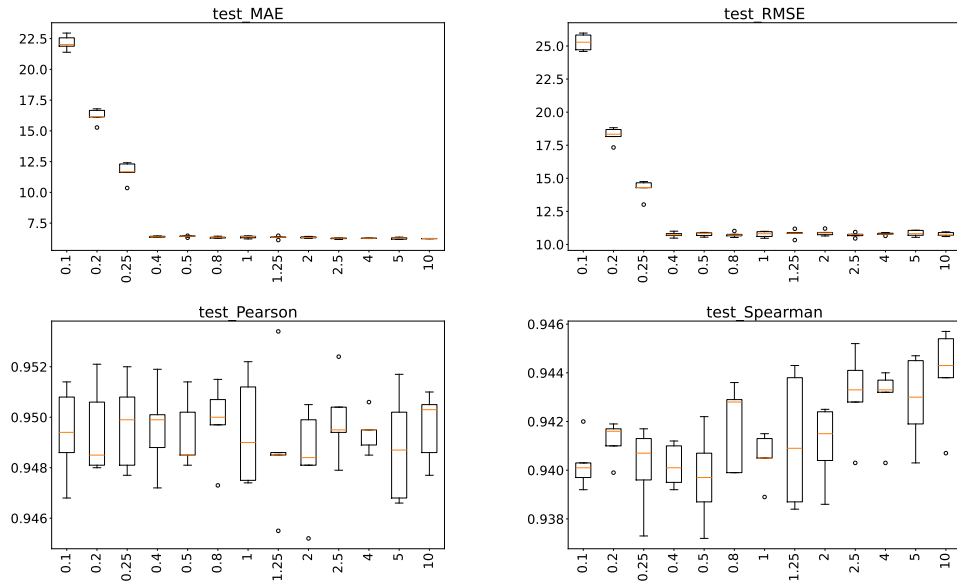


Figure 8: Different α (x-axis) for FAR on Super Conductivity.

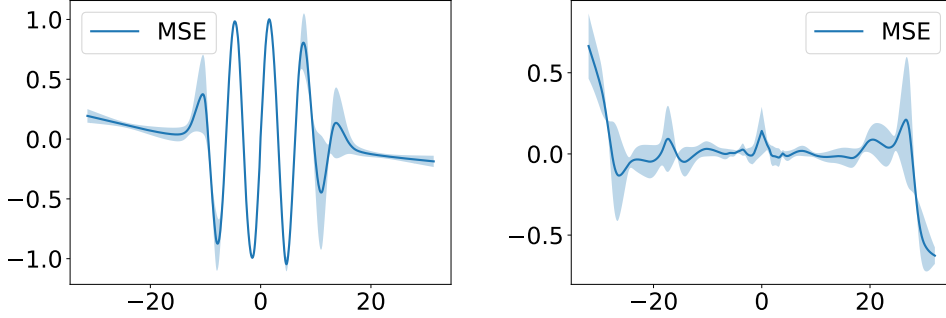


Figure 9: MSE predictions on synthetic datasets.

B.3 Experiment Settings for AgeDB

We follow the the same experiment settings from the previous work (Zha et al., 2023). The SGD optimizer and cosine learning rate annealing is utilized for training (Loshchilov and Hutter, 2016). The batch size is set to 256. For both training from scratch and linear probe experiments, we select the best learning rates and weight decays for each dataset by grid search, with a grid of learning rates from $\{0.01, 0.05, 0.1, 0.2, 0.5, 1.0\}$ and weight decays from $\{1e-6, 1e-5, 1e-4, 1e-3\}$. For the predictor training of two-stage methods, we adopt the same search setting as above except for adding no weight decay to the search choices of weight decays. The RNC temperature parameter is search from $\{0.1, 0.2, 0.5, 1.0, 2.0, 5.0\}$ and select the best, which is 2.0. We train all one-stage methods and the encoder of two-stage methods for 400 epochs, and the linear regressor of two-stage methods for 100 epochs. The hyper-parameters for all the compared methods are searched in the same region as described in the main content. For training from scratch experiments, because the ConR (Keramati et al., 2023) is proposed to use two data augmentations, we utilize two data augmentations for each training data for all comparied baselines.

B.4 Data Pre-processing for IC50

For IC50 (Garnett et al., 2012), there are some missing values for all the 130 drugs across all tumour cell lines, which make the model training and evaluation inconvenient. We filter out the drugs with more than 28% missing values, which gives us targets for 15 drugs. Then, we filter the data samples (cell lines) that don’t have any missing values for the 15 drugs, which end up with 429 samples. We utilize dummy variables to encode data categorical features (tissue type, cancer type, genetic information).

B.5 MSE on Synthetic Datasets

Due to the limited space and high similarity between MAE and MSE, we include the predictions for MSE in Fig. 9. As mentioned in the main content and Fig. 1, 2, MSE is similar with MAE, which performs worse on fitting function derivatives/shapes than the proposed FAR.

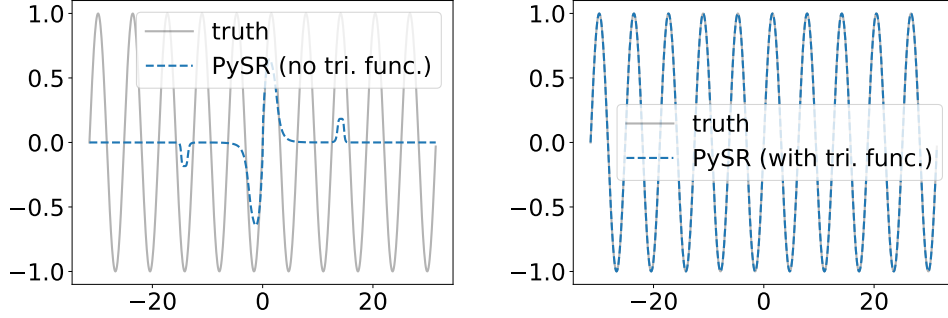


Figure 10: PySR on Sine dataset.

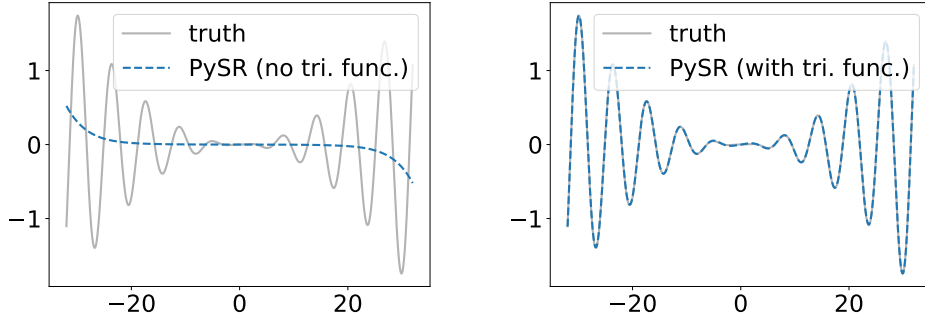


Figure 11: PySR on Squared Sine dataset.

B.6 Symbolic Regression on the Synthetic Datasets

We adopt PySR (Cranmer, 2023) on the synthetic experiments. We present the results for without trigonometric functions and with trigonometric functions prior knowledge in Fig 10 and Fig. 11 for Sine and Squared Sine datasets. The predictions (dashed line) is the mean prediction values based on 5 independent runs of PySR.

B.7 Backbone Model Complexity Variation on Sine Dataset

To demonstrate the effectiveness for the proposed FAR. We varies the backbone model complexity from $\{2,4,6,8,10\}$ hidden layers for the previous FFNN backbone model, besides of the previous 5 hidden layers FFNN results in the main content. α for FAR is tuned in $\{0.5,1,2\}$. All of other settings are kept the same as previously described in the main content. The results are presented in the Fig 12. Based on the results, we have two observations: 1) increasing model complexity can generally improve the learning performance but may saturate at certain level (e.g. for MAE, 8 hidden layers model is better than 10 hidden layers model; for MSE, 6 hidden layers model is better 8 and 10 hidden layers model). 2) FAR consistently demonstrates its superiority over other baseline methods for comparison.

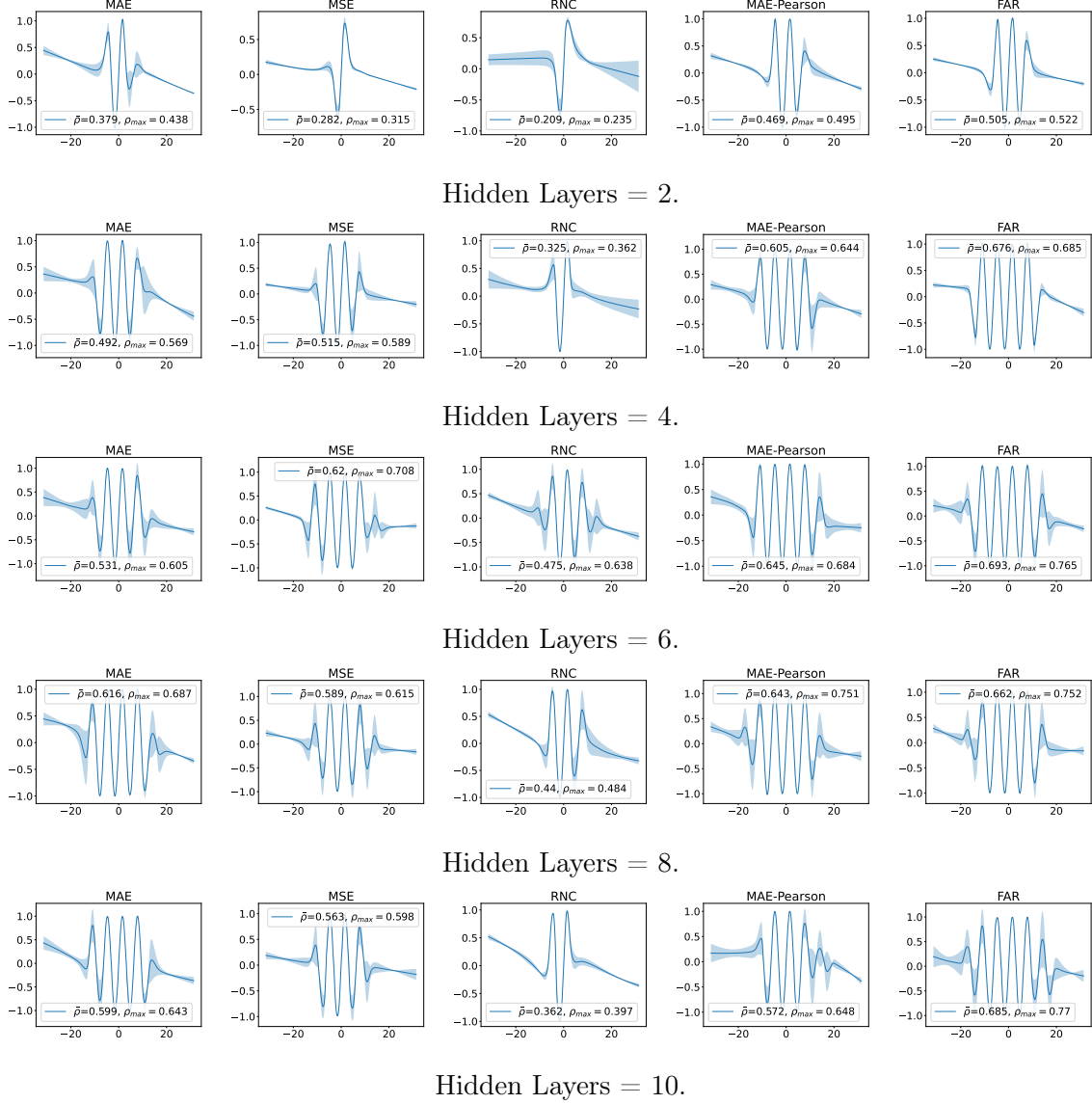


Figure 12: Predictions from different numbers of hidden layers for FFNN on Sine dataset. $\bar{\rho}$ stands for the averaged Pearson correlation coefficient with the ground truth over the 5 trials; ρ_{\max} is the maximal Pearson correlation coefficient with the ground truth over the 5 trials.

B.8 Ablation Study on FAR

Recall that FAR constitutes of three sub-losses: conventional MAE loss $\mathcal{L}_c^{\text{MAE}}$, the MSE derivative loss $\mathcal{L}_{\text{diff}}^{\text{MSE}}$, the normalized derivative loss with p-norm (p=2), that is $\mathcal{L}_{\text{diffnorm}}^{p=2}$. Therefore, we conduct the similar experiments for the extra six variants of FAR on the tabular datasets as an ablation study. The results are summarized in Tab. 4. From the results, we observe that the proposed FAR with all the three components performs the best over all the variants.

Table 4: FAR constitutes of 3 different sub-losses; thereby there are 6 variants for ablation study on FAR by taking off the components. \downarrow means the smaller the better; \uparrow means the larger the better. Mean and standard deviation (in the parenthesis) values are reported. The overall ranks for each variant are reported in the last row.

Dataset	Method	$\mathcal{L}_c^{\text{MAE}}$	$\mathcal{L}_{\text{diff}}^{\text{MSE}}$	$\mathcal{L}_{\text{diffnorm}}^{p=2}$	$\mathcal{L}_c^{\text{MAE}}$ and $\mathcal{L}_{\text{diff}}^{\text{MSE}}$	$\mathcal{L}_c^{\text{MAE}}$ and $\mathcal{L}_{\text{diffnorm}}^{p=2}$	$\mathcal{L}_{\text{diff}}^{\text{MSE}}$ and $\mathcal{L}_{\text{diffnorm}}^{p=2}$	FAR
Wine Quality	MAE \downarrow	0.631(0.008)	1.251(0.722)	1.587(0.799)	0.609(0.009)	0.611(0.002)	1.206(0.211)	0.596(0.002)
	RMSE \downarrow	0.821(0.012)	1.425(0.686)	1.914(0.746)	0.771(0.006)	0.786(0.006)	1.42(0.22)	0.756(0.005)
	Pearson \uparrow	0.346(0.043)	0.507(0.004)	0.507(0.008)	0.461(0.013)	0.503(0.009)	0.5(0.018)	0.503(0.007)
	Spearman \uparrow	0.385(0.014)	0.514(0.004)	0.519(0.008)	0.467(0.022)	0.518(0.008)	0.513(0.018)	0.511(0.009)
Abalone	MAE \downarrow	1.505(0.018)	8.81(0.29)	7.167(1.798)	1.493(0.012)	1.494(0.019)	7.235(2.707)	1.494(0.016)
	RMSE \downarrow	2.174(0.017)	9.115(0.31)	7.987(1.473)	2.161(0.011)	2.164(0.029)	7.595(2.568)	2.147(0.014)
	Pearson \uparrow	0.736(0.003)	0.743(0.006)	0.741(0.004)	0.746(0.003)	0.742(0.008)	0.74(0.005)	0.748(0.003)
	Spearman \uparrow	0.77(0.004)	0.777(0.004)	0.776(0.005)	0.776(0.004)	0.778(0.003)	0.777(0.004)	0.778(0.004)
Parkinson (Total)	MAE \downarrow	3.358(0.045)	27.563(0.902)	24.393(2.48)	2.746(0.068)	2.648(0.13)	26.861(0.707)	2.64(0.071)
	RMSE \downarrow	5.384(0.05)	28.306(1.115)	26.489(1.795)	4.214(0.14)	4.402(0.253)	27.363(1.036)	4.258(0.206)
	Pearson \uparrow	0.866(0.002)	0.934(0.012)	0.951(0.004)	0.924(0.005)	0.912(0.01)	0.939(0.011)	0.922(0.009)
	Spearman \uparrow	0.846(0.003)	0.922(0.012)	0.942(0.004)	0.911(0.006)	0.897(0.013)	0.931(0.011)	0.907(0.01)
Parkinson (Motor)	MAE \downarrow	2.277(0.075)	19.211(0.571)	16.788(0.811)	1.672(0.085)	1.853(0.174)	19.188(0.707)	1.652(0.069)
	RMSE \downarrow	3.927(0.036)	19.687(0.583)	19.373(0.752)	2.701(0.131)	3.116(0.361)	19.709(0.938)	2.68(0.134)
	Pearson \uparrow	0.875(0.002)	0.942(0.009)	0.944(0.003)	0.942(0.005)	0.919(0.022)	0.943(0.009)	0.943(0.006)
	Spearman \uparrow	0.868(0.002)	0.939(0.009)	0.94(0.004)	0.938(0.007)	0.913(0.024)	0.94(0.009)	0.939(0.006)
Super Conductivity	MAE \downarrow	6.577(0.051)	20.445(0.88)	14.27(0.631)	6.293(0.072)	6.238(0.051)	18.616(1.762)	6.257(0.027)
	RMSE \downarrow	11.815(0.114)	23.676(0.778)	17.094(0.607)	10.719(0.178)	10.935(0.042)	21.514(1.661)	10.745(0.183)
	Pearson \uparrow	0.94(0.001)	0.95(0.002)	0.947(0.001)	0.95(0.002)	0.948(0.0)	0.951(0.001)	0.949(0.002)
	Spearman \uparrow	0.942(0.001)	0.942(0.001)	0.939(0.002)	0.943(0.001)	0.945(0.001)	0.942(0.001)	0.944(0.002)
IC50	MAE \downarrow	1.359(0.002)	3.815(0.009)	3.549(0.044)	1.369(0.006)	1.362(0.012)	3.736(0.021)	1.359(0.003)
	RMSE \downarrow	1.709(0.012)	4.134(0.011)	3.87(0.044)	1.706(0.003)	1.705(0.018)	4.053(0.02)	1.7(0.005)
	Pearson \uparrow	0.041(0.045)	0.146(0.022)	0.293(0.034)	0.07(0.062)	0.313(0.023)	0.313(0.021)	0.302(0.028)
	Spearman \uparrow	0.085(0.035)	0.152(0.034)	0.267(0.019)	0.115(0.031)	0.268(0.009)	0.263(0.029)	0.26(0.024)
Overall	Rank	5.312	5.146	4.229	3.354	3.125	4.458	2.375

References

- Ramzi Benkraiem and Constantin Zopounidis. Preface: Regression methods based on or techniques and computational aspects in management, economics and finance. *Annals of Operations Research*, 306:1–6, 2021.
- Ting Chen, Simon Kornblith, Mohammad Norouzi, and Geoffrey Hinton. A simple framework for contrastive learning of visual representations. In *International conference on machine learning*, pages 1597–1607. PMLR, 2020.
- Lorenzo Ciampiconi, Adam Elwood, Marco Leonardi, Ashraf Mohamed, and Alessandro Rozza. A survey and taxonomy of loss functions in machine learning. *arXiv preprint arXiv:2301.05579*, 2023.
- Djork-Arné Clevert, Thomas Unterthiner, and Sepp Hochreiter. Fast and accurate deep network learning by exponential linear units (elus). *arXiv preprint arXiv:1511.07289*, 2015.

- Paulo Cortez, António Cerdeira, Fernando Almeida, Telmo Matos, and José Reis. Modeling wine preferences by data mining from physicochemical properties. *Decision support systems*, 47(4):547–553, 2009.
- Miles Cranmer. Interpretable machine learning for science with pysr and symbolicregression.jl. *arXiv preprint arXiv:2305.01582*, 2023.
- Suresh Dara, Swetha Dhamercherla, Surender Singh Jadav, CH Madhu Babu, and Mohamed Jawed Ahsan. Machine learning in drug discovery: a review. *Artificial Intelligence Review*, 55(3):1947–1999, 2022.
- Y Dodge. Least absolute deviation regression. *The Concise Encyclopedia of Statistics*, pages 299–302, 2008.
- Mathew J Garnett, Elena J Edelman, Sonja J Heidorn, Chris D Greenman, Anahita Dastur, King Wai Lau, Patricia Greninger, I Richard Thompson, Xi Luo, Jorge Soares, et al. Systematic identification of genomic markers of drug sensitivity in cancer cells. *Nature*, 483(7391):570–575, 2012.
- Yu Gong, Greg Mori, and Fred Tung. Ranksim: Ranking similarity regularization for deep imbalanced regression. In *International Conference on Machine Learning*, pages 7634–7649. PMLR, 2022.
- Kam Hamidieh. Superconductivity Data. UCI Machine Learning Repository, 2018. DOI: <https://doi.org/10.24432/C53P47>.
- Sepp Hochreiter and Jürgen Schmidhuber. Long short-term memory. *Neural computation*, 9(8):1735–1780, 1997.
- David Holzmüller, Viktor Zaverkin, Johannes Kästner, and Ingo Steinwart. A framework and benchmark for deep batch active learning for regression. *Journal of Machine Learning Research*, 24(164):1–81, 2023.
- Peter J Huber. Robust estimation of a location parameter. In *Breakthroughs in statistics: Methodology and distribution*, pages 492–518. Springer, 1992.
- Mahsa Keramati, Lili Meng, and R David Evans. Conr: Contrastive regularizer for deep imbalanced regression. *arXiv preprint arXiv:2309.06651*, 2023.
- Diederik P Kingma and Jimmy Ba. Adam: A method for stochastic optimization. *arXiv preprint arXiv:1412.6980*, 2014.
- Adrien Marie Legendre. *Nouvelles méthodes pour la détermination des orbites des comètes: avec un supplément contenant divers perfectionnemens de ces méthodes et leur application aux deux comètes de 1805*. Courcier, 1806.
- Ilya Loshchilov and Frank Hutter. Sgdr: Stochastic gradient descent with warm restarts. *arXiv preprint arXiv:1608.03983*, 2016.

- Stylianos Moschoglou, Athanasios Papaioannou, Christos Sagonas, Jiankang Deng, Irene Kotsia, and Stefanos Zafeiriou. Agedb: the first manually collected, in-the-wild age database. In *proceedings of the IEEE conference on computer vision and pattern recognition workshops*, pages 51–59, 2017.
- Warwick Nash, Tracy Sellers, Simon Talbot, Andrew Cawthorn, and Wes Ford. Abalone. UCI Machine Learning Repository, 1995. DOI: <https://doi.org/10.24432/C55C7W>.
- Zhenxing Niu, Mo Zhou, Le Wang, Xinbo Gao, and Gang Hua. Ordinal regression with multiple output cnn for age estimation. In *Proceedings of the IEEE conference on computer vision and pattern recognition*, pages 4920–4928, 2016.
- Scott Pesme and Nicolas Flammarion. Online robust regression via sgd on the l1 loss. *Advances in Neural Information Processing Systems*, 33:2540–2552, 2020.
- Brenden K Petersen, Mikel Landajuela, T Nathan Mundhenk, Claudio P Santiago, Soo K Kim, and Joanne T Kim. Deep symbolic regression: Recovering mathematical expressions from data via risk-seeking policy gradients. *arXiv preprint arXiv:1912.04871*, 2019.
- Jiawei Ren, Mingyuan Zhang, Cunjun Yu, and Ziwei Liu. Balanced mse for imbalanced visual regression. In *Proceedings of the IEEE/CVF Conference on Computer Vision and Pattern Recognition*, pages 7926–7935, 2022.
- Rasmus Rothe, Radu Timofte, and Luc Van Gool. Dex: Deep expectation of apparent age from a single image. In *Proceedings of the IEEE international conference on computer vision workshops*, pages 10–15, 2015.
- Walter Rudin et al. *Principles of mathematical analysis*, volume 3. McGraw-hill New York, 1976.
- David E Rumelhart, Geoffrey E Hinton, and Ronald J Williams. Learning representations by back-propagating errors. *nature*, 323(6088):533–536, 1986.
- Matthieu Solnon, Sylvain Arlot, and Francis Bach. Multi-task regression using minimal penalties. *The Journal of Machine Learning Research*, 13(1):2773–2812, 2012.
- Valentin Stanev, Corey Oses, A Gilad Kusne, Efrain Rodriguez, Johnpierre Paglione, Stefano Curtarolo, and Ichiro Takeuchi. Machine learning modeling of superconducting critical temperature. *npj Computational Materials*, 4(1):29, 2018.
- Robert Tibshirani. Regression shrinkage and selection via the lasso. *Journal of the Royal Statistical Society Series B: Statistical Methodology*, 58(1):267–288, 1996.
- Andrey Nikolayevich Tikhonov et al. On the stability of inverse problems. In *Dokl. akad. nauk sssr*, volume 39, pages 195–198, 1943.
- Athanasios Tsanas, Max Little, Patrick McSharpy, and Lorraine Ramig. Accurate telemonitoring of parkinson’s disease progression by non-invasive speech tests. *Nature Precedings*, pages 1–1, 2009.

- Ashish Vaswani, Noam Shazeer, Niki Parmar, Jakob Uszkoreit, Llion Jones, Aidan N Gomez, Łukasz Kaiser, and Illia Polosukhin. Attention is all you need. *Advances in neural information processing systems*, 30, 2017.
- Denny Wu and Ji Xu. On the optimal weighted ℓ_2 regularization in overparameterized linear regression. *Advances in Neural Information Processing Systems*, 33:10112–10123, 2020.
- Yuzhe Yang, Kaiwen Zha, Yingcong Chen, Hao Wang, and Dina Katabi. Delving into deep imbalanced regression. In *International Conference on Machine Learning*, pages 11842–11851. PMLR, 2021.
- Kaiwen Zha, Peng Cao, Jeany Son, Yuzhe Yang, and Dina Katabi. Rank-n-contrast: Learning continuous representations for regression. In *Thirty-seventh Conference on Neural Information Processing Systems*, 2023.
- Shihao Zhang, Linlin Yang, Michael Bi Mi, Xiaoxu Zheng, and Angela Yao. Improving deep regression with ordinal entropy. *arXiv preprint arXiv:2301.08915*, 2023.
- Dixian Zhu, Changjie Cai, Tianbao Yang, and Xun Zhou. A machine learning approach for air quality prediction: Model regularization and optimization. *Big data and cognitive computing*, 2(1):5, 2018.
- Dixian Zhu, Yiming Ying, and Tianbao Yang. Label distributionally robust losses for multi-class classification: Consistency, robustness and adaptivity. In *International Conference on Machine Learning*, pages 43289–43325. PMLR, 2023.
- Hui Zou. The adaptive lasso and its oracle properties. *Journal of the American statistical association*, 101(476):1418–1429, 2006.
- Hui Zou and Trevor Hastie. Regularization and variable selection via the elastic net. *Journal of the Royal Statistical Society Series B: Statistical Methodology*, 67(2):301–320, 2005.